Massless objects dynamics in star clusters

fmfd@uni-heidelberg.de

Francesco Flammini Dotti

20 August 2024
CAMK, Warsaw

Outline

- Why massless objects are interesting?
- How can we study large Ns systems?
- Ejection from the planetary systems in star clusters
- Mass segregation and massless objects
- General conclusions

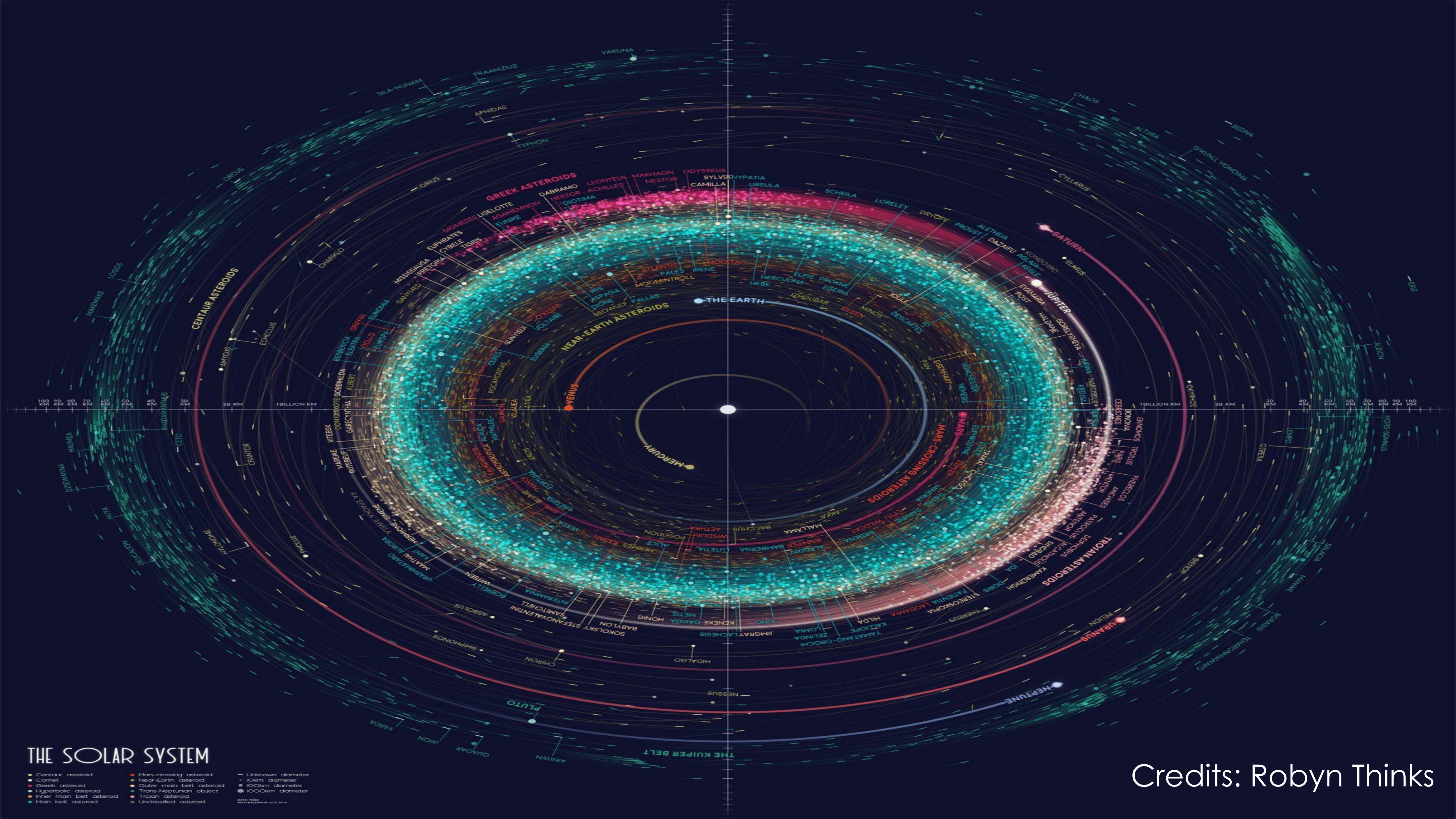

Credits: Robyn Thinks

Planets: 8
Dwarf Planets: 5
Moons: > 200
Comets: > 4 000
Asteroids: > 10^6

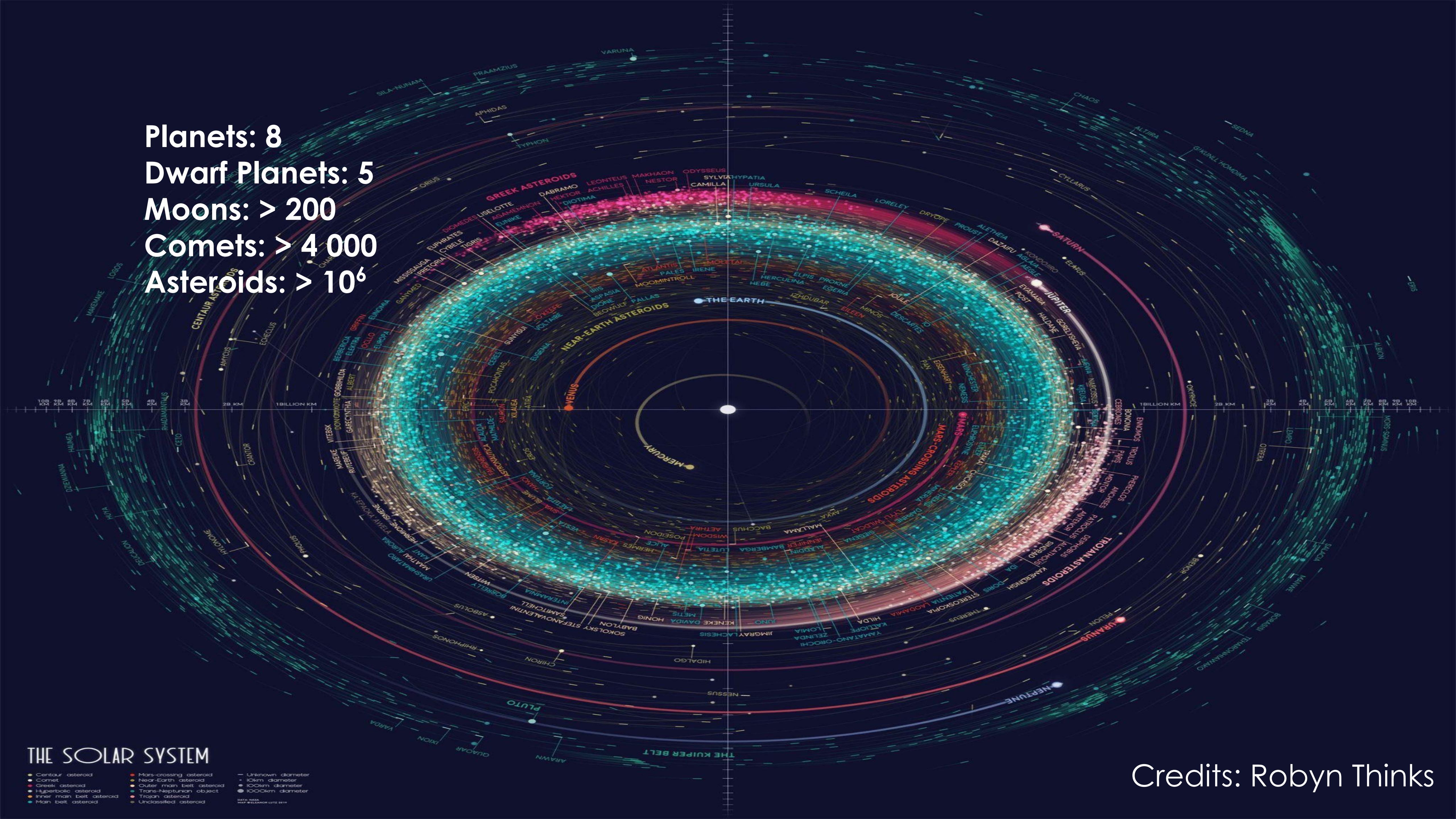

Credits: Robyn Thinks

Planets: 8
Dwarf Planets: 5
Moons: > 200
Comets: > 4 000
Asteroids: > 10^6

Multiply for the estimated number of stars in the MW:

Planets: 4×10^{11}
Moons: > $8\ 10^{13}$
Comets: > $1.6\ 10^{15}$
Asteroids: > $4\ 10^{17}$

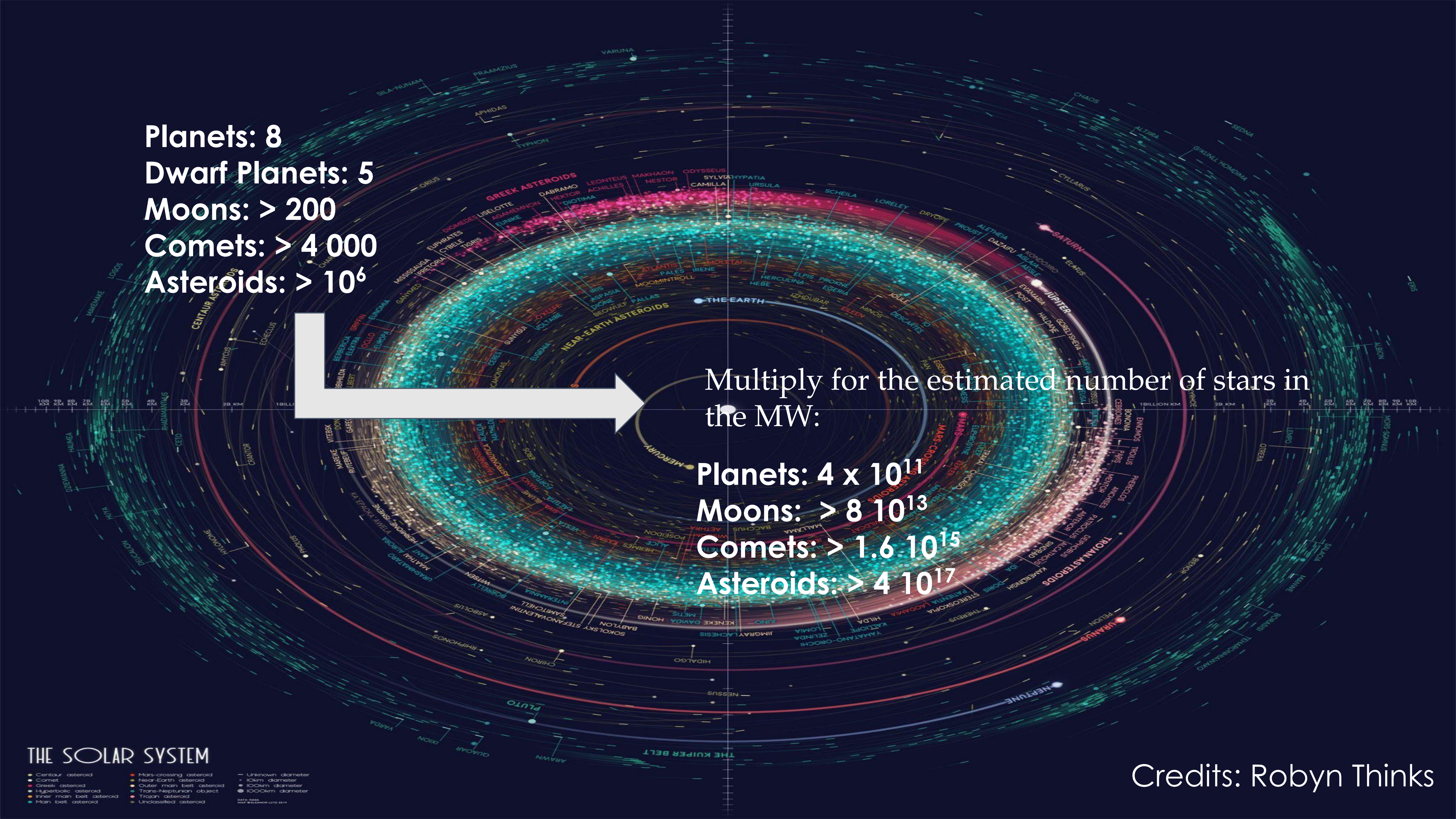

Credits: Robyn Thinks

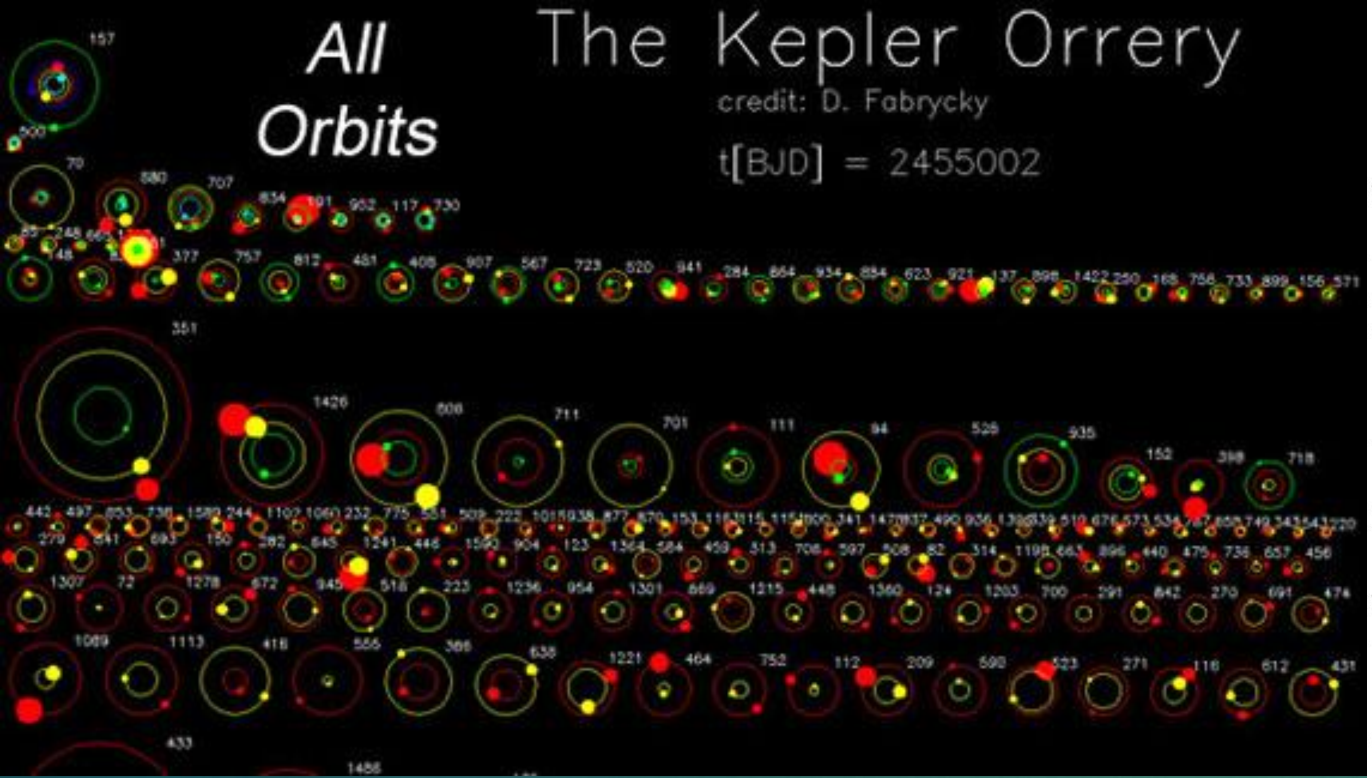

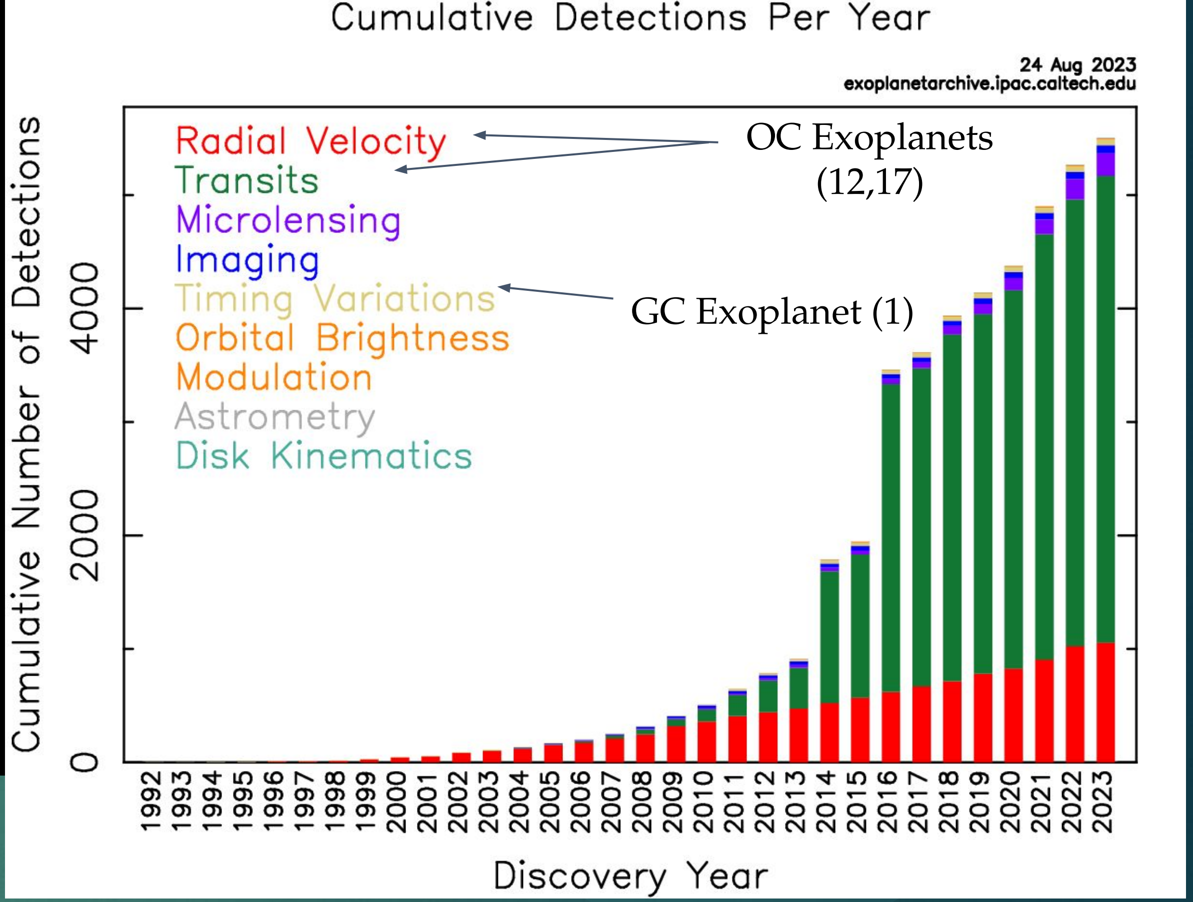

- Open clusters only recently we managed to have observations! Transit and radial velocity easier, microlensing also possible!
- Globular clusters and Young massive clusters: neighbours contaminate the samples. Very very difficult. We were very lucky with the discovery!

Brown Dwarf?
Large semi-major axis?
Globulette?
In star cluster??

Stars estimation in MW: 2-4 10^{11} stars
FFPs estimation in MW: 0.5-1 10^{11} ffp

Gahm 2013

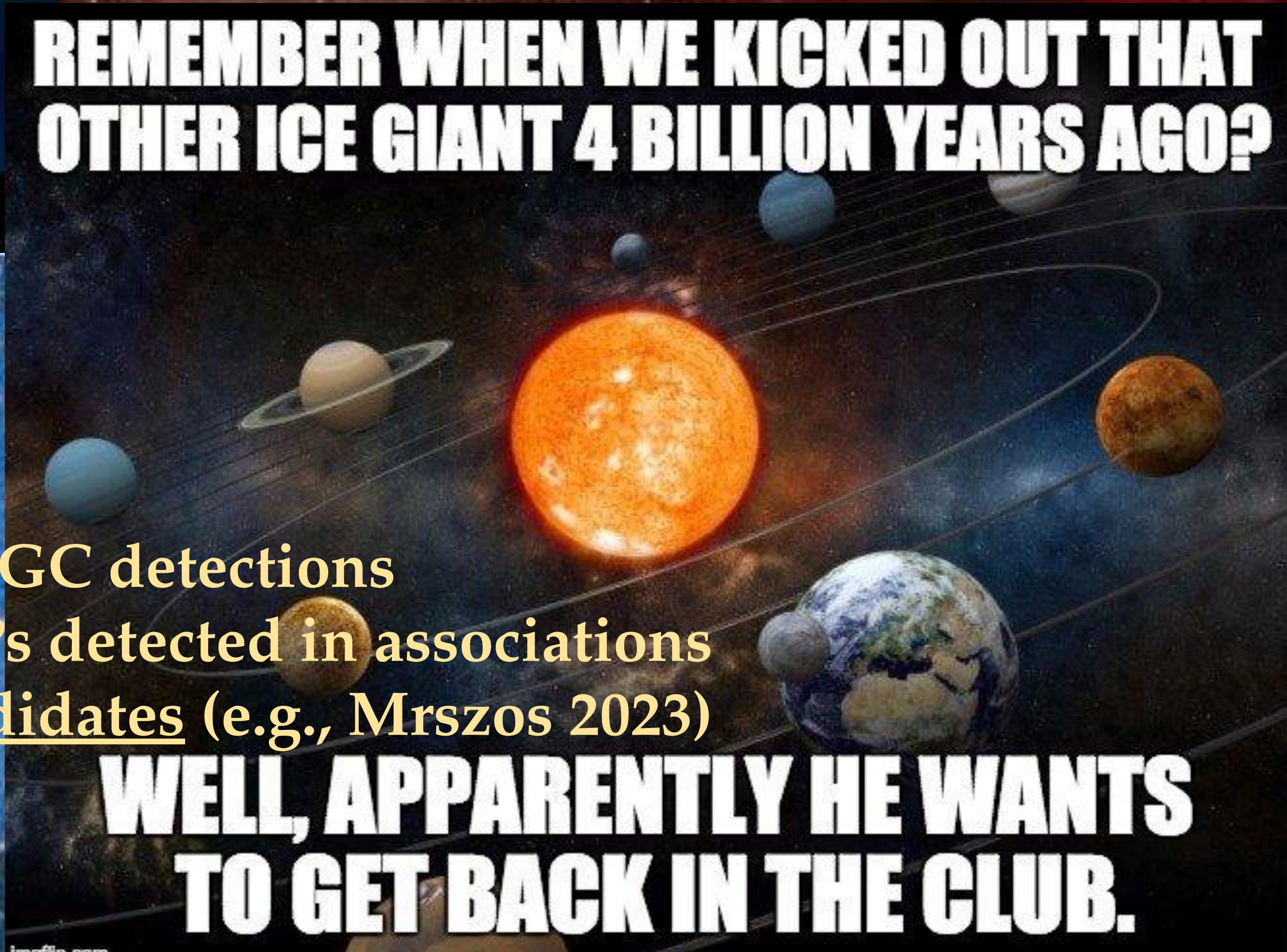

No OC or GC detections
Only 2 confirmed FFPs detected in associations
Many, many FFP candidates (e.g., Mrszos 2023)

Miret-Roig 2023

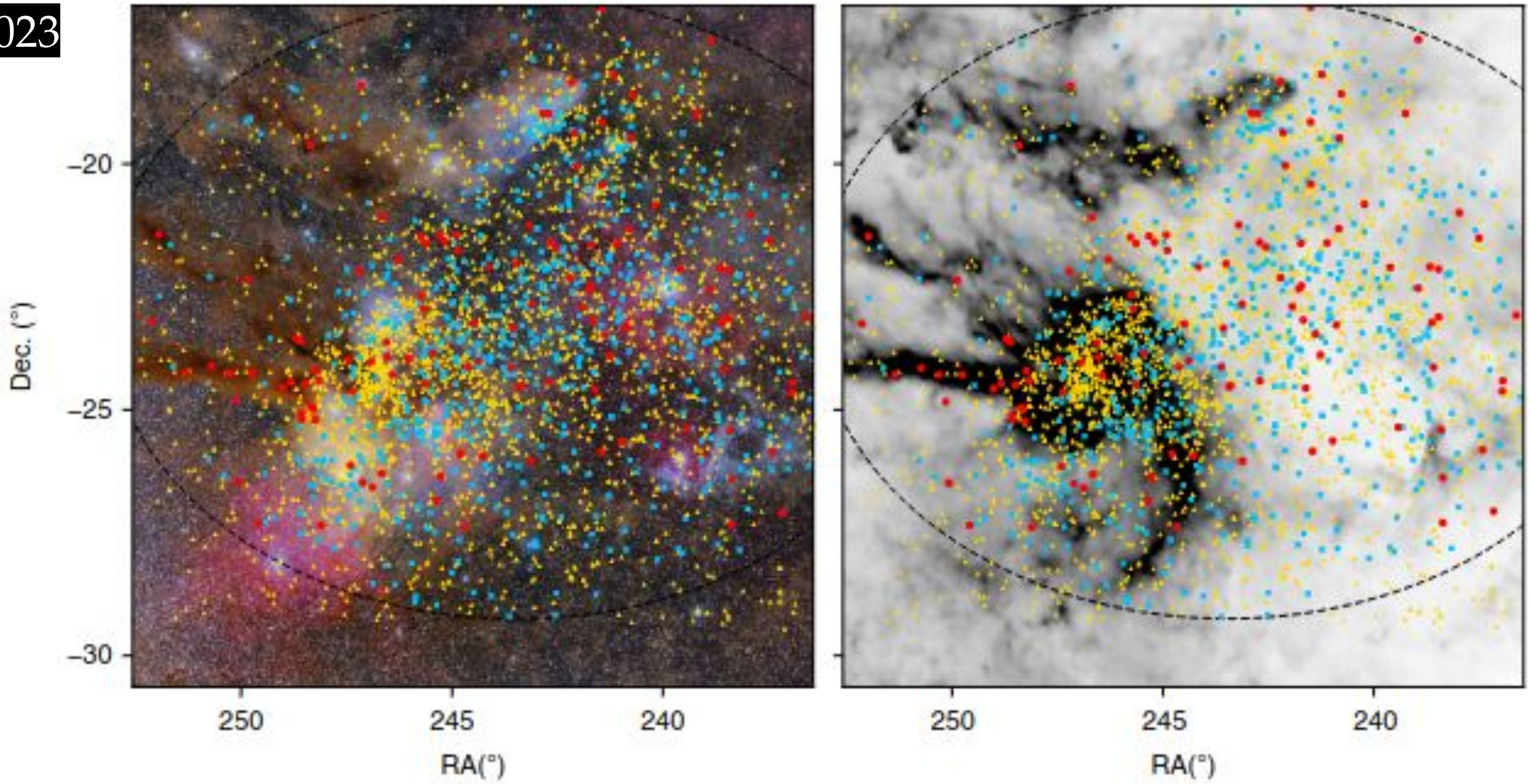

Fig. 1 | Sky distribution of stars, brown dwarfs and FFPs discovered in this study and classified assuming an age of 5 Myr. Stars are shown as yellow triangles, brown dwarfs as blue squares and FFPs as red dots. The dashed ellipses indicate the area analysed with the DANCe catalogue (Methods). The distributions are overlaid on background images taken in optical (left) and radio (right, at 857 GHz) wavelengths. Background images adapted with permission from: left, Mario Cogo (http://galaxlux.com); right, ref. [96], EDP Sciences.

Miret-Roig 2023

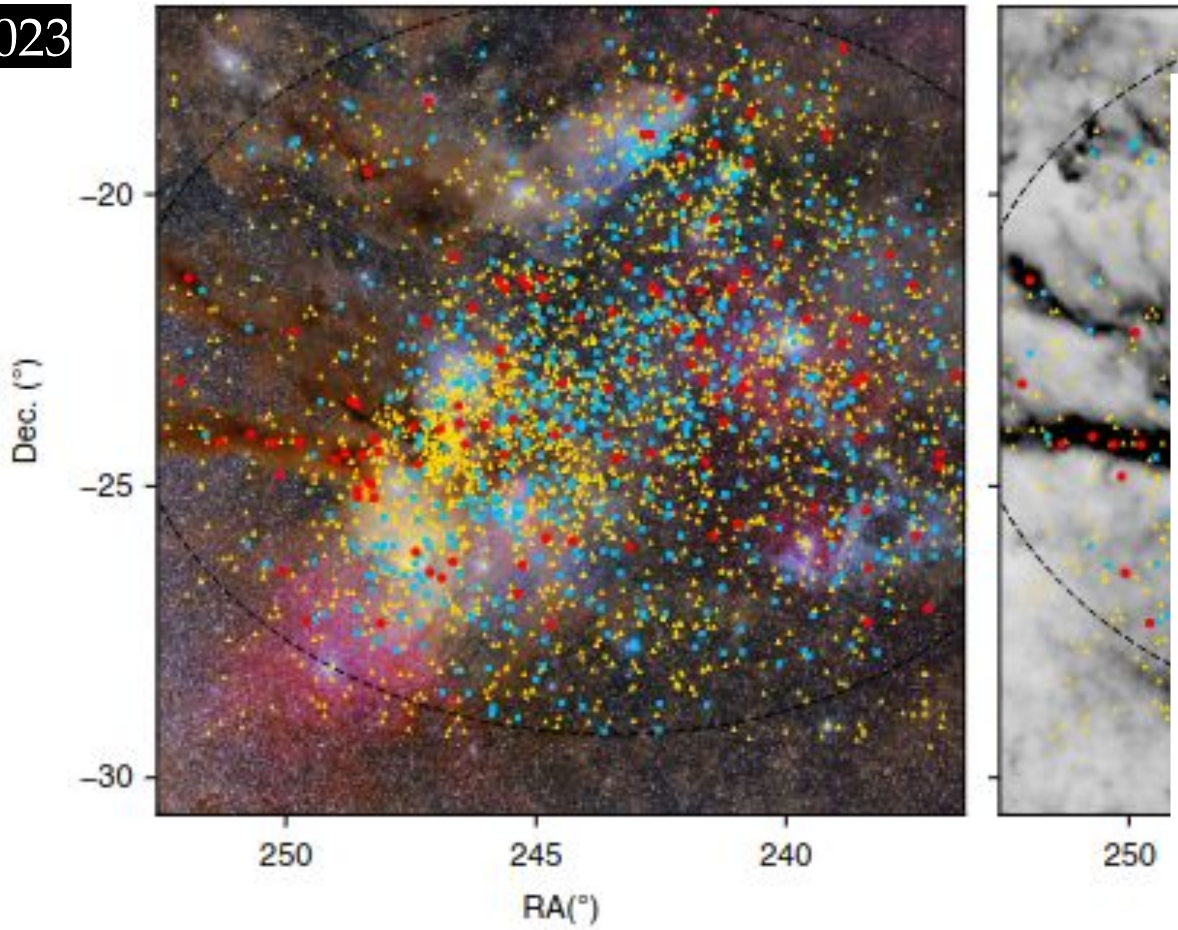

Fig. 1 | Sky distribution of stars, brown dwarfs and FFPs discovered in this study and classifie
triangles, brown dwarfs as blue squares and FFPs as red dots. The dashed ellipses indicate the
The distributions are overlaid on background images taken in optical (left) and radio (right, at
permission from: left, Mario Cogo (http://galaxlux.com); right, ref. [96], EDP Sciences.

Hurley and Shara 2002: FFP in SCs

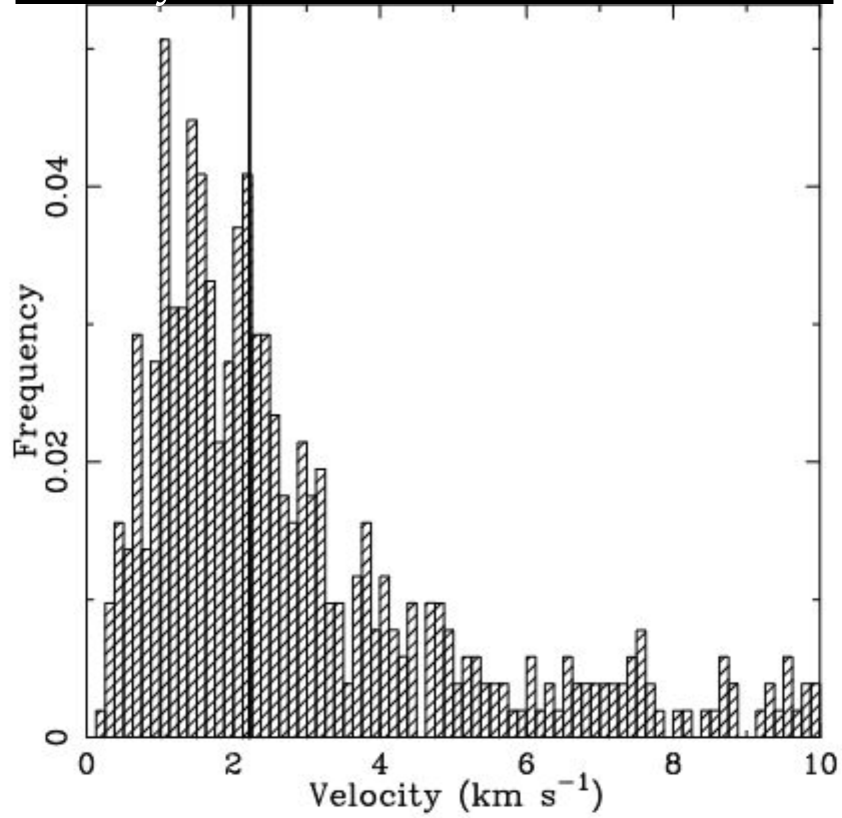

FIG. 3.—Distribution of velocities for free-floating planets immediately after being liberated from their parent star. Distribution is normalized to the total number of liberated planets. Average cluster escape velocity is also shown (*solid vertical line*): 46% of planets are liberated at speeds lower than the cluster escape velocity. Tail of distribution is truncated at 10 km s^{-1}, which excludes the 10% of the liberated planets with velocities extending out to 70 km s^{-1}.

Even after 1 Gyr, lots of ffp still in the cluster!

Methods for integrating planetary systems and star clusters

Direct method: stars and planets directly done by one code -> we use Nbody6++GPU (Kamlah et al 2022, Spurzem & Kamlah 2023) , Nbody6++GPU-ML (Flammini Dotti et al, submitted)

PRO: we can do everything on a single code
CON: Binary stars+planets and multiplanetary systems still not possible (or poorly implemented)

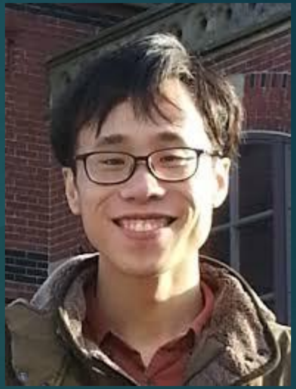

Indirect method: stars made by Nbody6++GPU o Nbody6++GPU-ML and then integrate planetary dynamics -> We use Lonely Planets (Cai 2019, Flammini Dotti 2019, Stock 2020, Benkendorff 2024), LonelyPlanets+ (Wu 2023, Wu et al, submitted) and Snipes (Flammini Dotti et al 2023)

PRO: We can do multiplanetary system, even adding debris disk and protoplanetary disks.
CON: slow, need external output

Computational performance of Nbody6++GPU-ML

Orange Lines 128k star cluster

Blue lines 64k star cluster

Total time in NBU = 10

Data by Han Solo@NAOC@Beijing

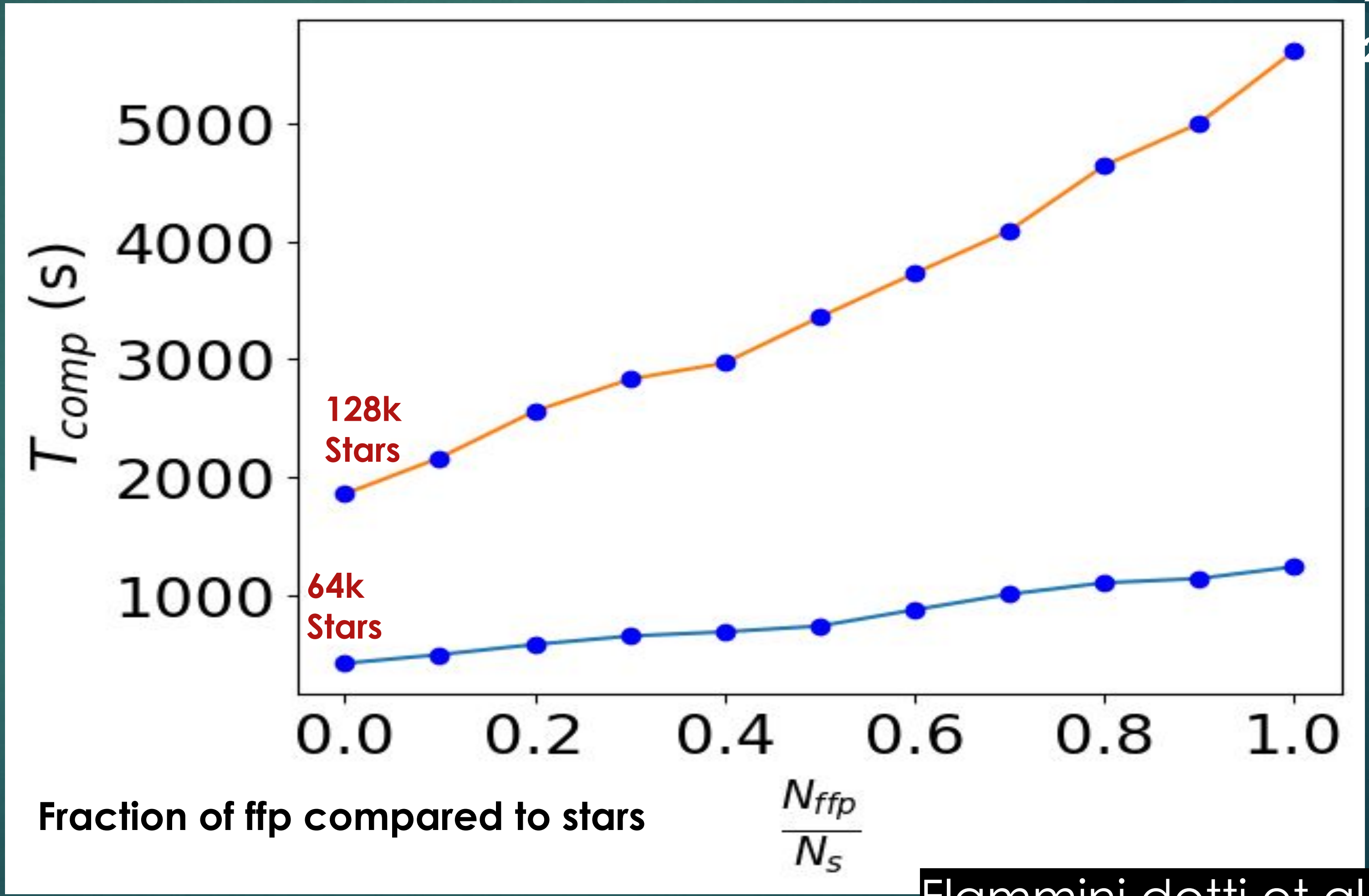

128k Stars+128k ffp
256k particles

64k Stars+64k Ffp
128k particles

Flammini dotti et al, submitted

Mass segregation and massless objects

Dynamical evolution of massless particles in star clusters with NBODY6++GPU-MASSLESS

I. Free-floating MLPs

Francesco Flammini Dotti*[1] , M.B.N. Kouwenhoven[2], Qi Shu[3,4] and Rainer Spurzem[1,5,3]

[1] Astronomisches Rechen-Institut, Zentrum für Astronomie, University of Heidelberg, Mönchhofstrasse 12–14, 69120, Heidelberg, Germany
[2] Department of Physics, School of Mathematics and Physics, Xi'an Jiaotong-Liverpool University, 111 Ren'ai Road, Suzhou Dushu Lake Science and Education Innovation District, Suzhou Industrial Park, Suzhou 215123, P.R. China
[3] Kavli Institute for Astronomy and Astrophysics, Peking University, Yiheyuan Lu 5, Haidian Qu, 100871, Beijing, China
[4] Department of Astronomy, School of Physics, Peking University, Yiheyuan Lu 5, Haidian Qu, 100871, Beijing, China
[5] National Astronomical Observatories and Key Laboratory of Computational Astrophysics, Chinese Academy of Sciences, 20A Datun Rd., Chaoyang District, 100101, Beijing, China

Received –; accepted –

ABSTRACT

Context. MLPs, such as comets, asteroids, planetesimals, and free-floating planets, are continuously injected into the intra-cluster environment after expulsion from their host planetary systems. However their dynamics, in large numbers, has rarely been carefully studied
Aims. We investigate the dynamical evolution of MLP populations in star clusters, and characterize their kinematics and ejection rates.
Methods. We present NBODY6++GPU-MASSLESS, a modified version of the *N*-body simulation code NBODY6++GPU that allows fast integration of star clusters that contain large numbers of massless particles (MLPs). This version of NBODY6++GPU contains routines especially directed for the dynamical evolution of planets
Results. Unlike stars, MLPs do not participate in the mass segregation process. Instead, MLPs mostly follow the gravitational potential of the star cluster, which gradually decreases over time due to stellar ejections and stellar evolution. The dynamical evolution of MLPs is primarily affected by the evolution of stellar core of the star cluster. This is most apparent in the outer regions for clusters with higher initial densities. High escape rates of MLPs are observed before the core-collapse, after which escape rates remain stable. Denser star clusters support the earlier assumption that stars undergo more intense core collapse, but this does not impact the dynamical evolution of MLPs. Finally, the speeds of escaping stars are similar to those of escaping MLPs, if we remove the high energy ejection of neutron stars during the first 50 Myr.

Initial conditions

Table 1. Initial conditions of the star cluster models.

Model	C12.8k	C64.8k	C128k
Number of stars, N_s	12 800	64 800	128 000
Number of MLPs,	12 800	64 800	128 000
Stellar initial mass function	Kroupa (2001), 0.08 – 150 $M_\odot$	Kroupa (2001), 0.08 – 150 $M_\odot$	Kroupa (2001), 0.08 – 150 $M_\odot$
MLP mass	Test particles	Test particles	Test particles
Total cluster mass, M_{cl}	$\sim 7.45 \times 10^3$ $M_\odot$	$\sim 3.7 \times 10^4$ $M_\odot$	$\sim 7.45 \times 10^4$ $M_\odot$
Dynamical model	Plummer (1911) model	Plummer (1911) model	Plummer (1911) model
MLP spatial distribution	Statistically identical to that of stars	Statistically identical to that of stars	Statistically identical to that of stars
MLP velocity distribution	Statistically identical to that of stars	Statistically identical to that of stars	Statistically identical to that of stars
Half-mass radius, r_{hm}	0.77 pc	0.77 pc	0.77 pc
Virial radius	1 pc	1 pc	1 pc
N-body (Hénon) time unit, T_*	0.18 Myr	0.08 Myr	0.06 Myr
Crossing time, t_{cr}	0.11 Myr	0.05 Myr	0.03 Myr
Half-mass relaxation time, t_{rh}	27.50 Myr	51.05 Myr	66.00 Myr
Stellar evolution	Mass loss enabled	Mass loss enabled	Mass loss enabled
External tidal force	Solar neighborhood	Solar neighborhood	Solar neighborhood
Simulation time	300 Myr	300 Myr	300 Myr

Stellar mass segregation

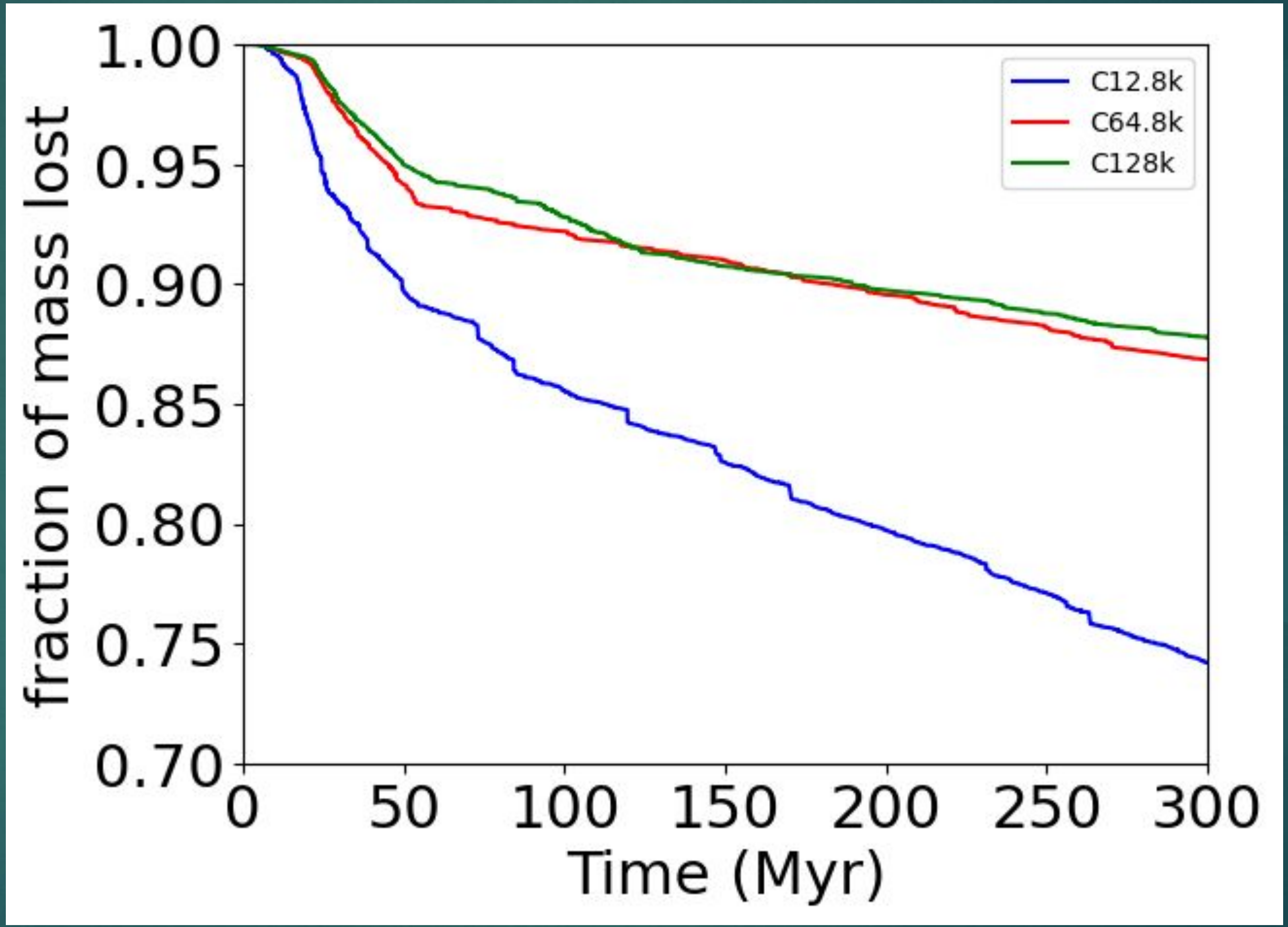

Stellar mass segregation

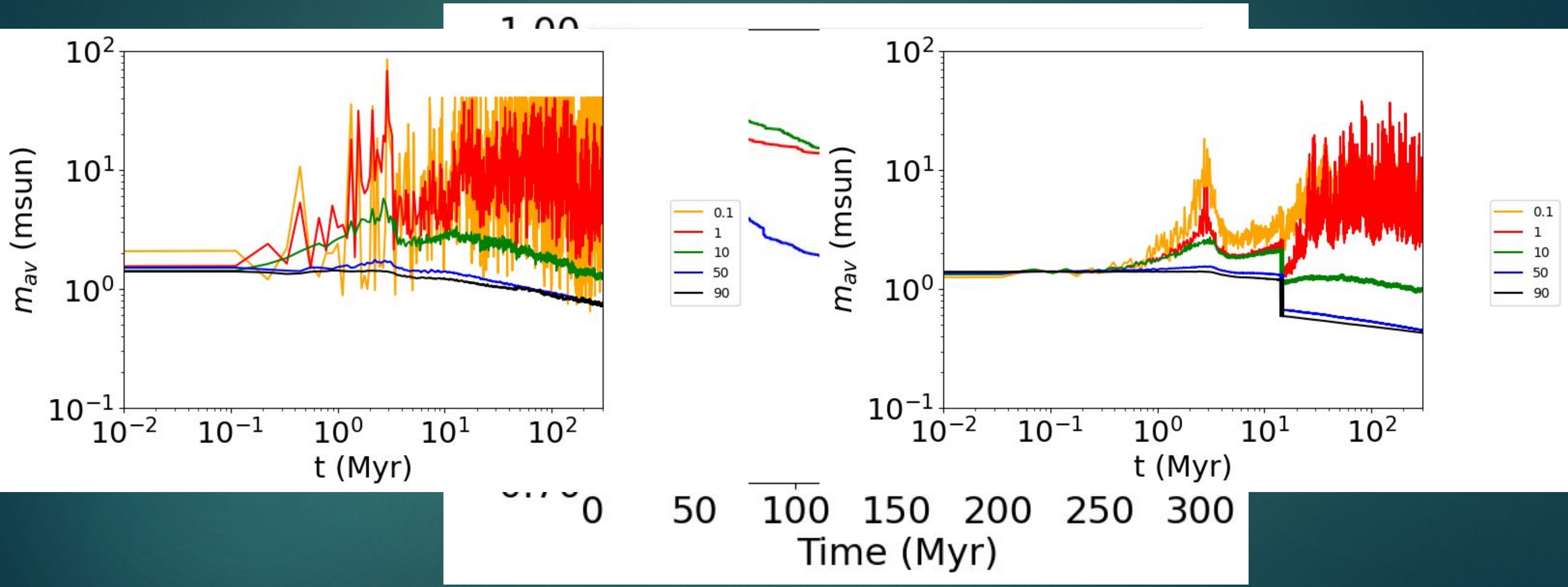

Inner regions Lagrangian radii

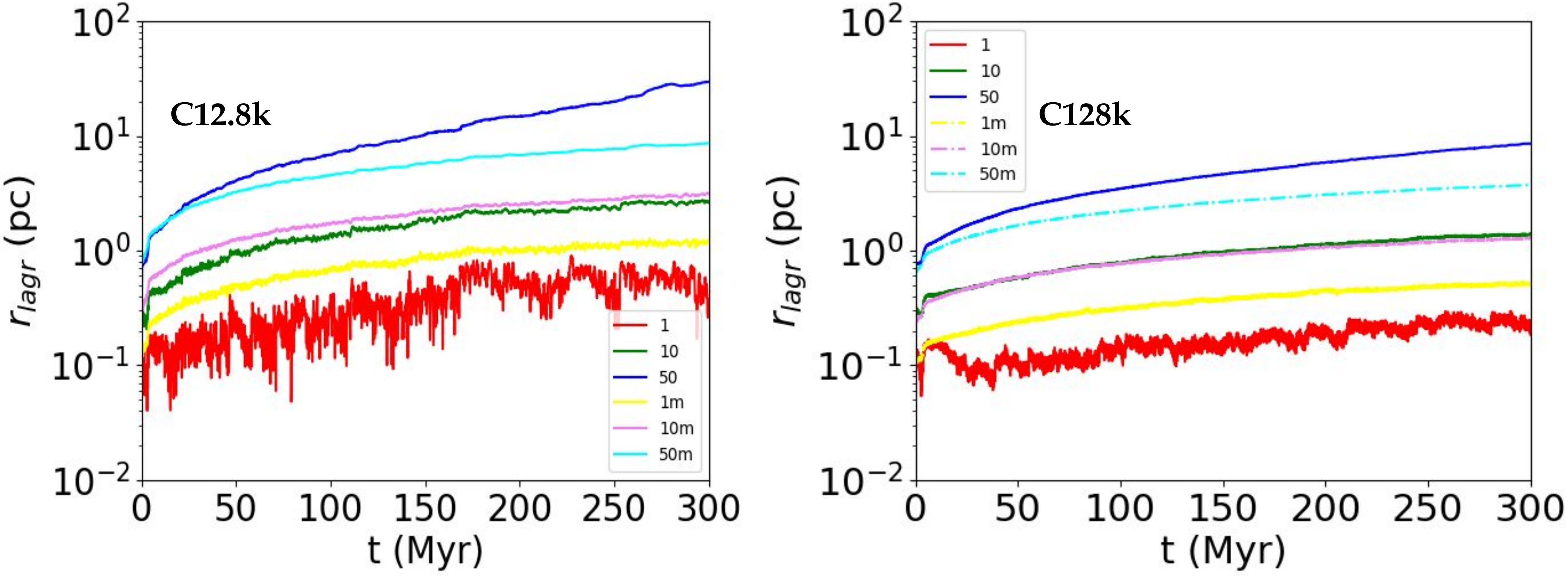

Inner regions larger massless Lagrangian radii — Larger densities reduce the gap, due to large encounter ratio

Half mass massless Lagrangian radius is smaller after a relaxation time, earlier in denser star clusters

All regions Lagrangian Radii

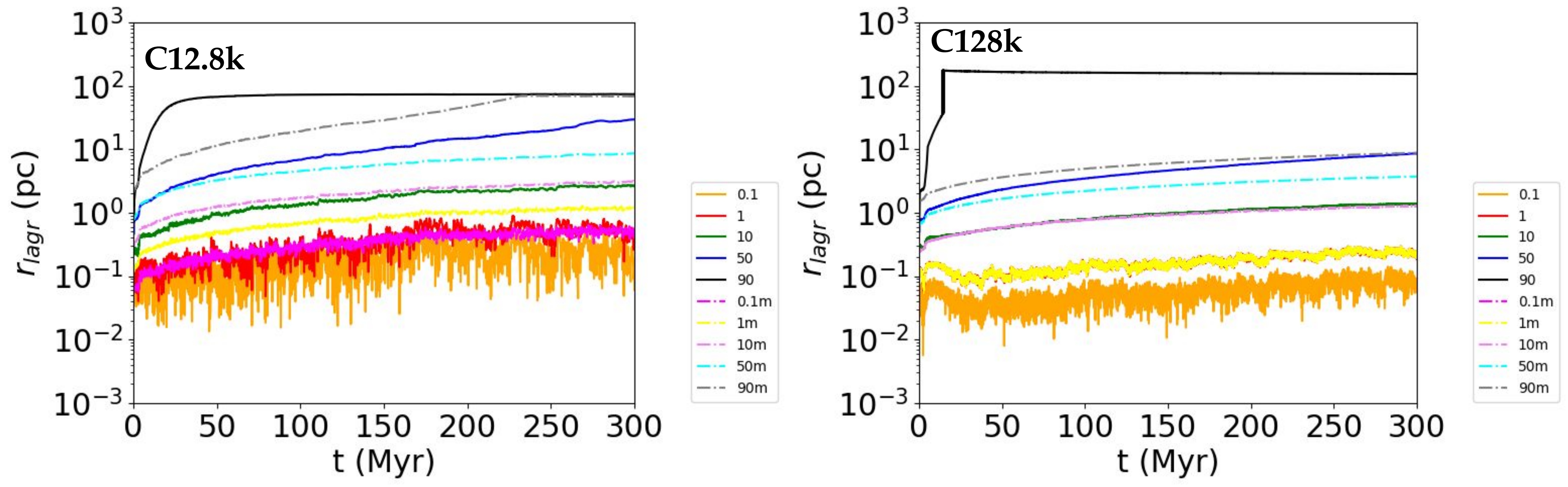

External regions of massless particles reach stars one after several relaxation times in C12.8k

External regions of massless is reached by the half-mass radii of the stars!

Cumulative distribution of ej. components

$\langle v_s \rangle$ = 3.86 km/s and 11.56 km/s $\langle v_{ffp} \rangle$ = 2.83 km/s and 9.41 km/s

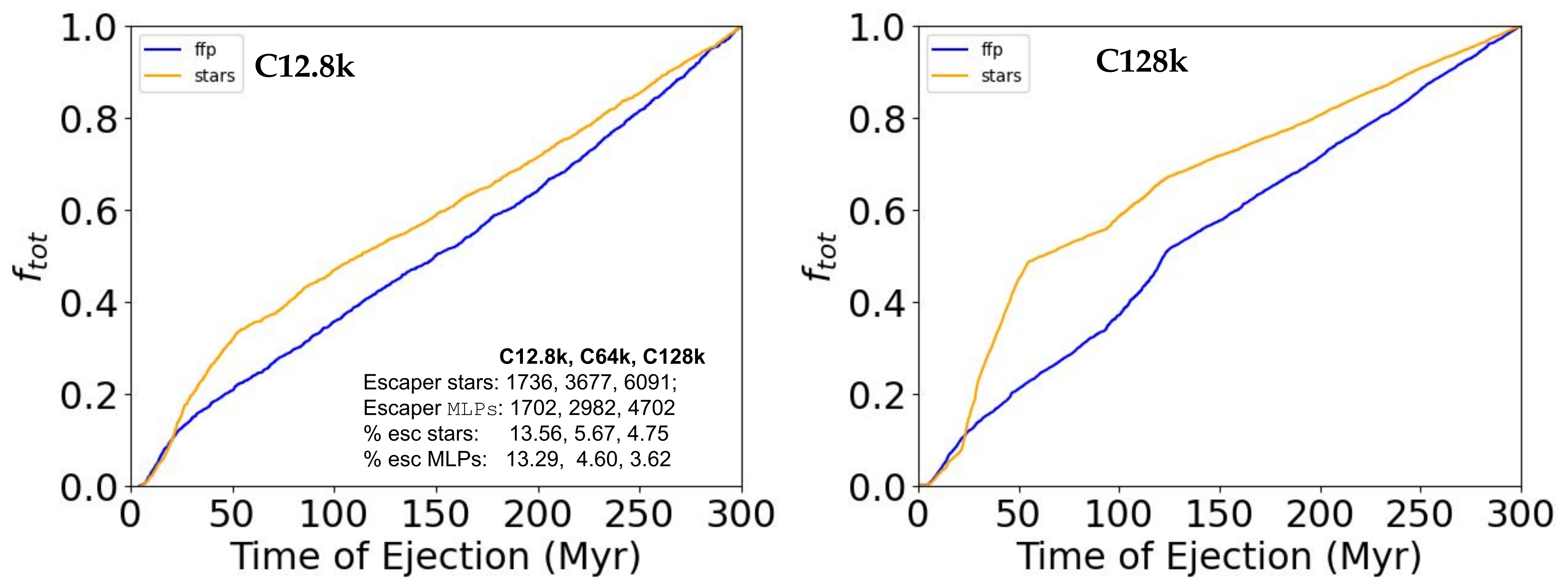

Escapers similar in less dense cluster, becomes larger in denser star cluster: the planets are bound to the core

General Conclusions

- The core plays a fundamental role in the earliest phases of star cluster evolution.
- The mass segregation do not impact massless objects evolution, only the core evolution does.
- The gravitational pull of the core is important for the massless particles
- Open and less dense clusters are more likely to eject ffps, denser cluster would retain ffps for many relaxation times

Future Outlook:

1) Varying massless energy distribution
2) Use a mass spectrum for massless planets
3) Million bodies simulations


Thanks for the attention!


Bonus slides!

Lagrangian radii with different distributions

$N_s = 10^4$; $N_{mlp} = 3\ 10^4$
r_{hm}=0.76 pc,

Stars are in virial equilibrium

Q=0.25,
Q=0.5,
Q = 0.75
for mlp

Escaped MLPs %:
59.71 % (17915)
57.27 % (17181)
60.00 % (18001)

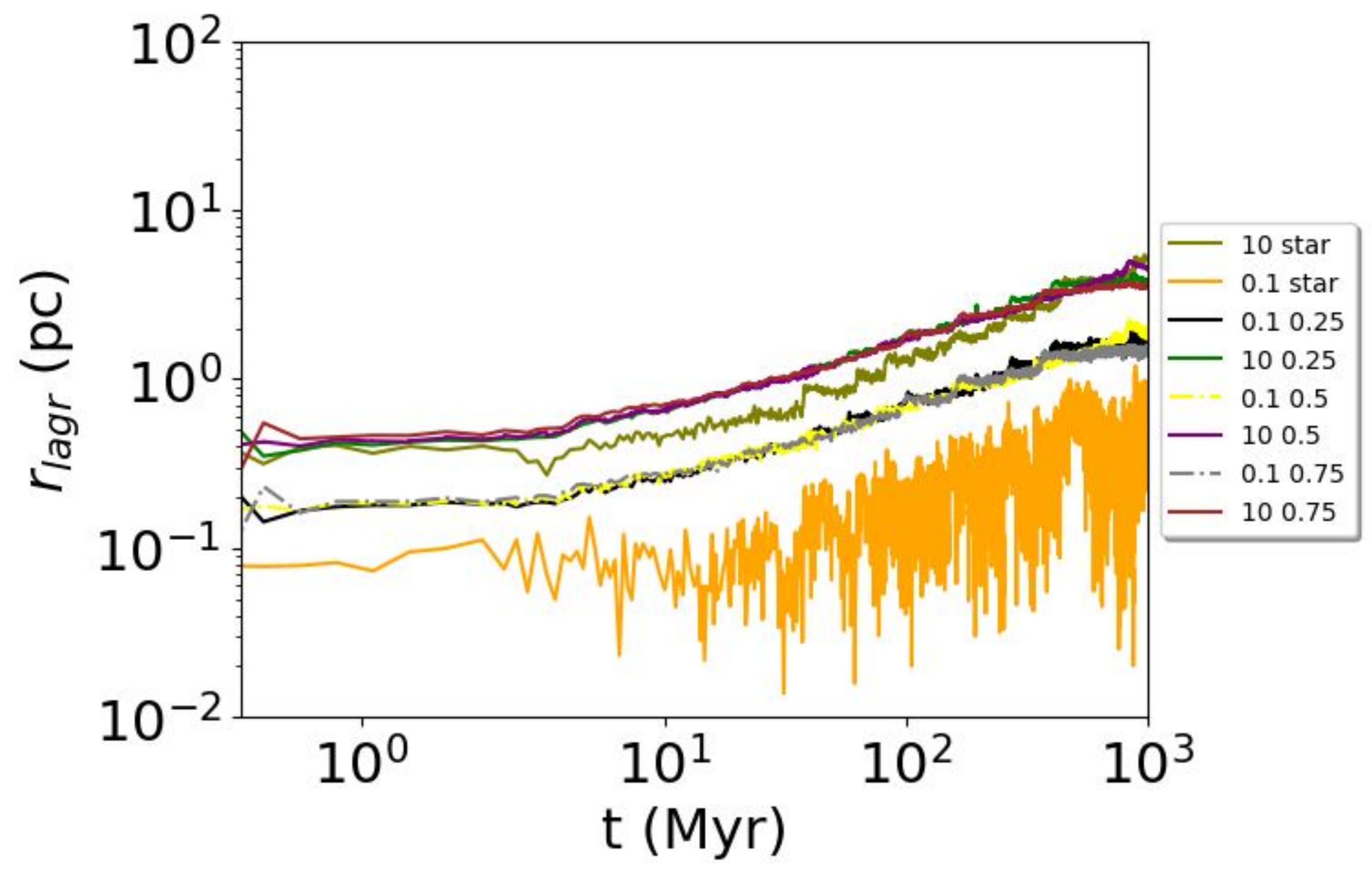

Lagrangian radii with different distributions

$N_s = 10^4$; $N_{mlp} = 3\ 10^4$
r_{hm}=0.76 pc,

Stars are in virial equilibrium

Q=0.25,
Q=0.5,
Q = 0.75
for mlp

Escaped MLPs %:
59.71 % (17915)
57.27 % (17181)
60.00 % (18001)

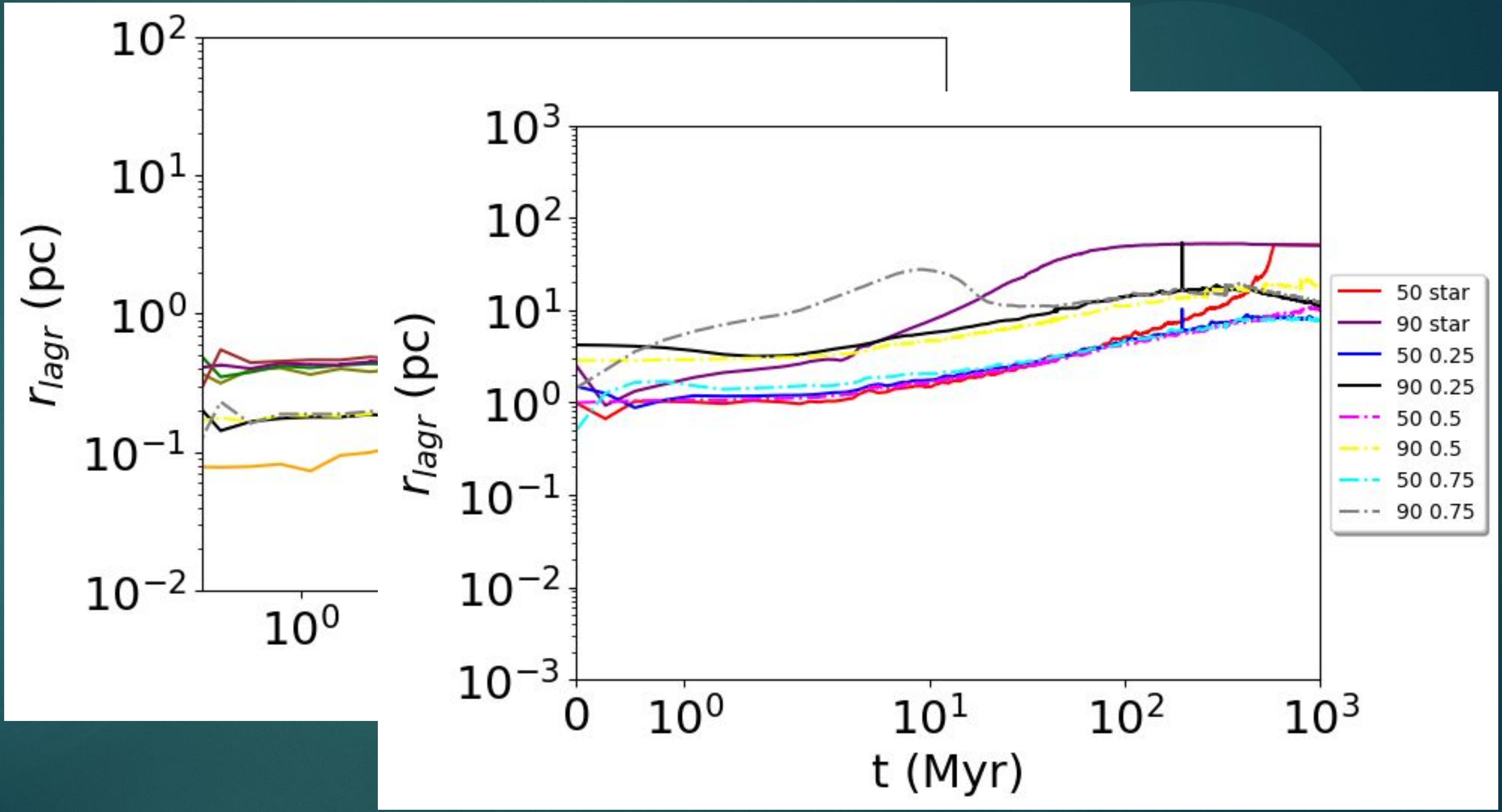

Types of encounters

- Adiabatic and non adiabatic encounters: $t_{enc} \gg t_{orb}$, otherwise non adiabatic
- Hyperbolic and near-parabolic encounters: hyperbolic when $e \geq 2$, while near-parabolic $1 < e < 2$ [Heggie 2006]
- Tidal and impulsive encounters: tidal when $p/a_p \geq 1$, impulsive when $p/a_p < 1$

$$\tilde{v}_\infty = v_\infty \left(\frac{G(m_{hp} + m_n)}{a_p} \right)^{-1/2}$$

$$k_p = \sqrt{\frac{2m_{hp}}{m_{hp} + m_n} \left(\frac{p}{a_p} \right)^3} \approx \left(\frac{p}{a_p} \right)^{3/2}$$

Encounter determination

<u>*EARTH*</u>

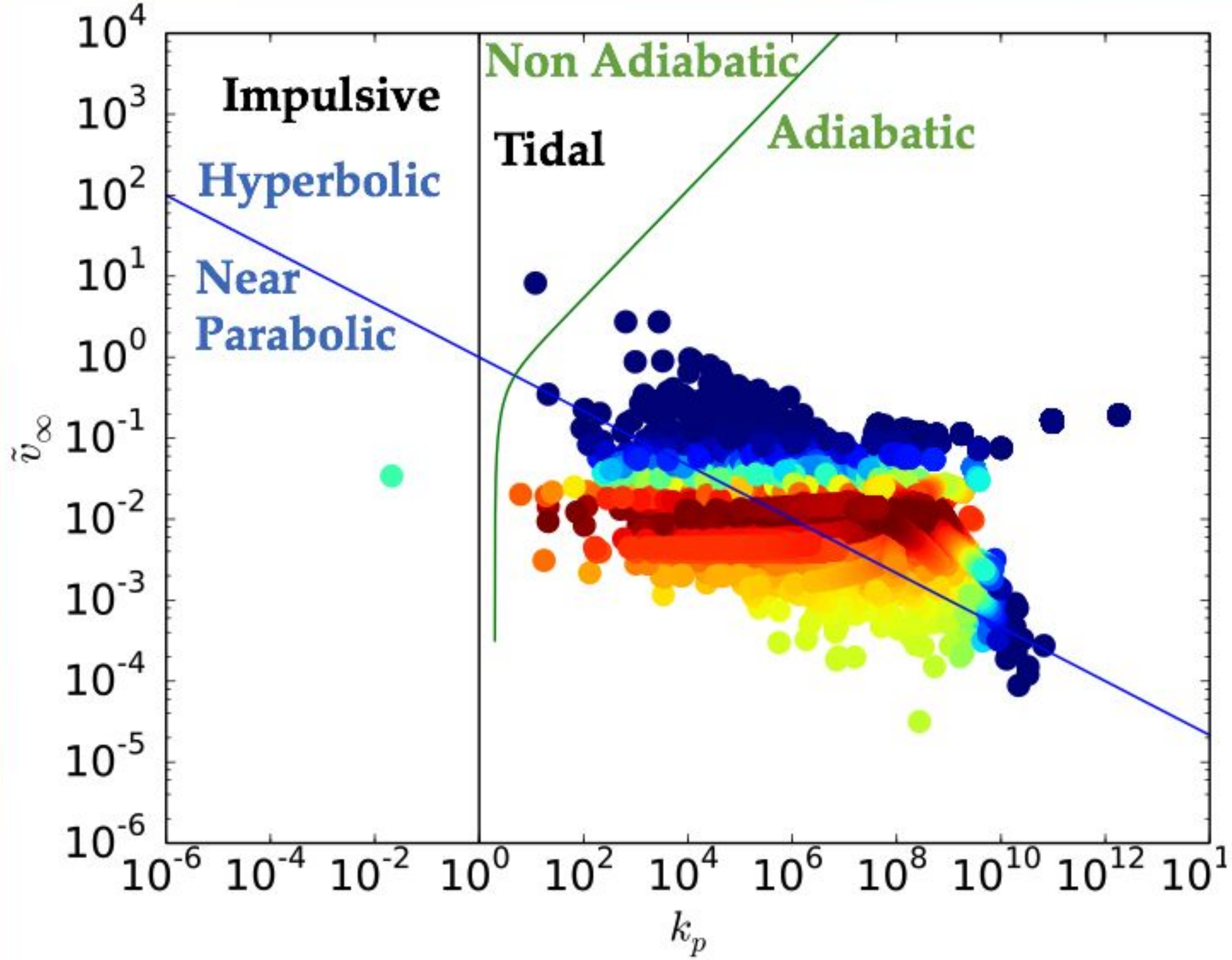

<u>*NEPTUNE*</u>

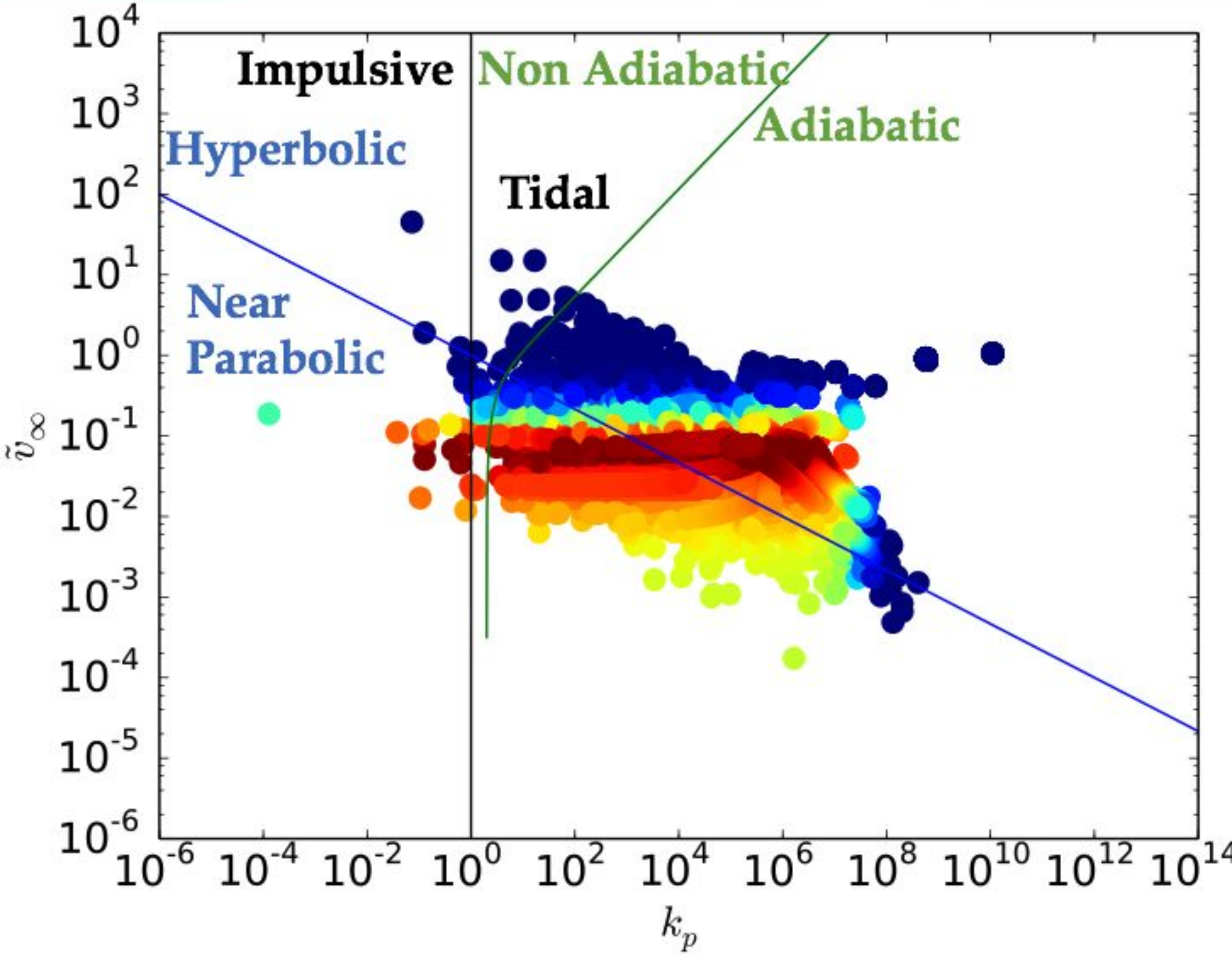

$$\tilde{v}_\infty = v_\infty \left(\frac{G(m_{hp} + m_n)}{a_p} \right)^{-1/2}$$

$$k_p = \sqrt{\frac{2m_{hp}}{m_{hp} + m_n} \left(\frac{p}{a_p} \right)^3} \approx \left(\frac{p}{a_p} \right)^{3/2}$$

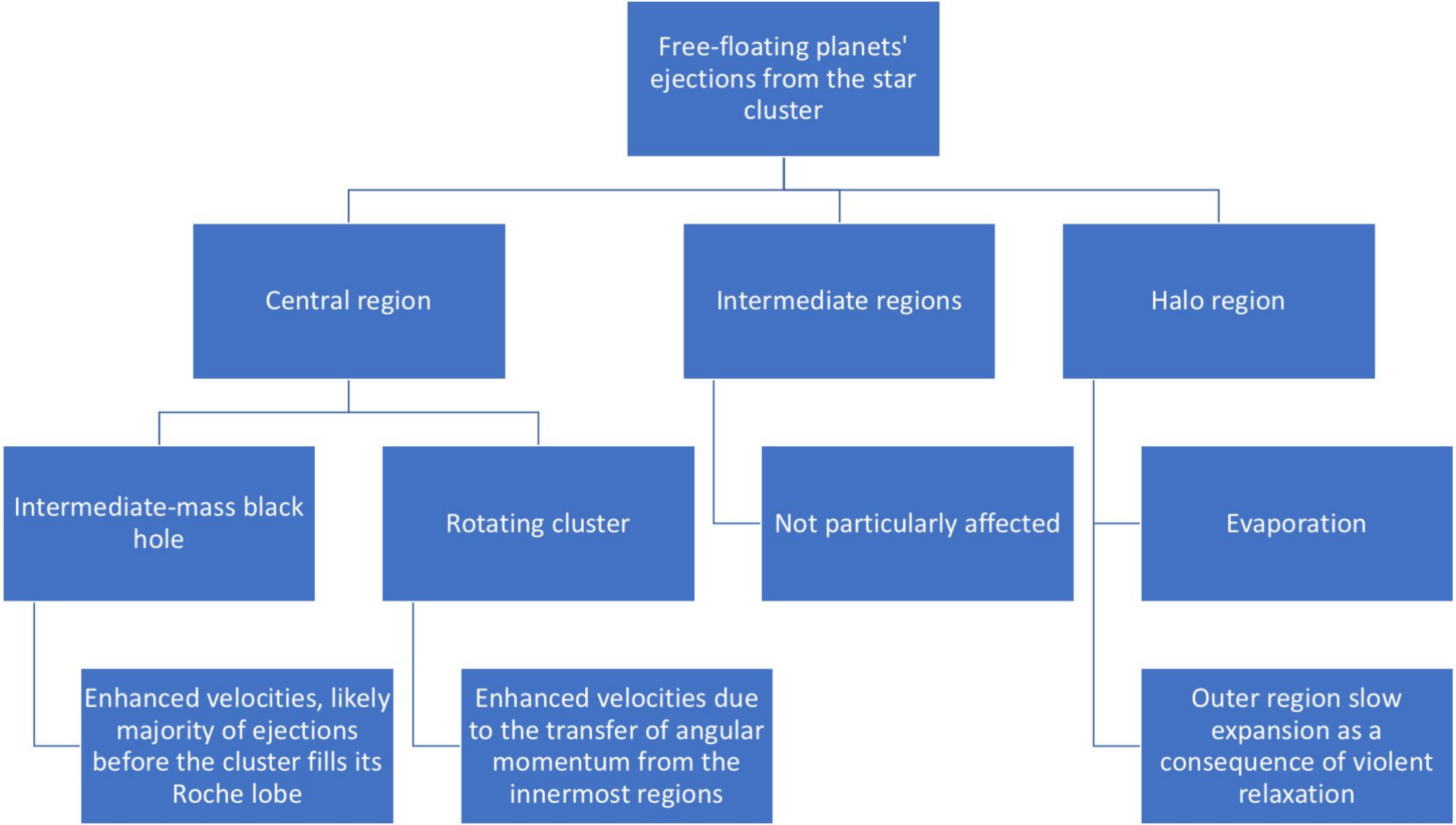
Free-floating planets' ejections from the star cluster
Central region
Intermediate regions
Halo region
Intermediate-mass black hole
Rotating cluster
Not particularly affected
Evaporation
Enhanced velocities, likely majority of ejections before the cluster fills its Roche lobe
Enhanced velocities due to the transfer of angular momentum from the innermost regions
Outer region slow expansion as a consequence of violent relaxation

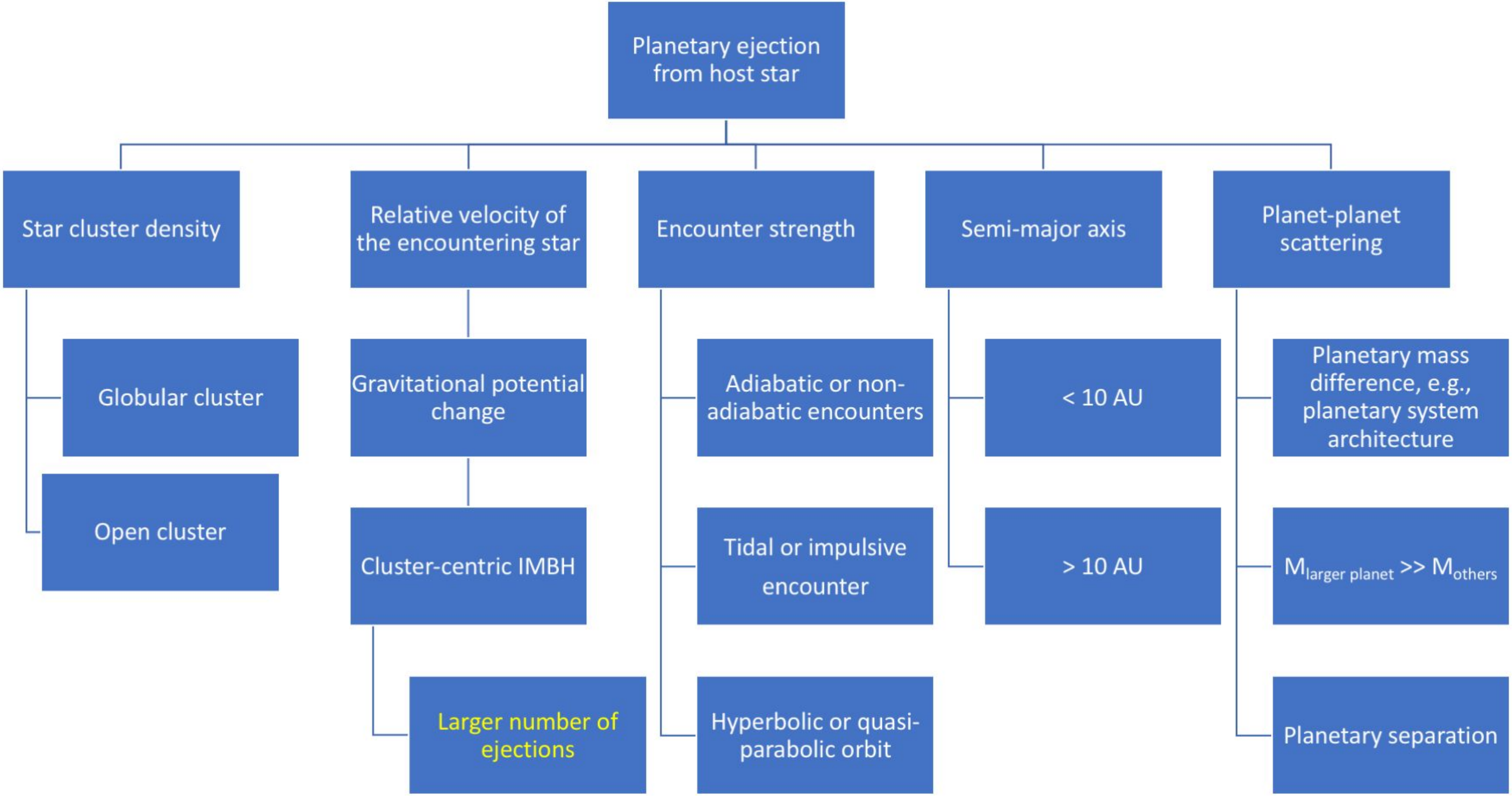

Planetary ejection from host star
Star cluster density
Relative velocity of the encountering star
Encounter strength
Semi-major axis
Planet-planet scattering
Globular cluster
Open cluster
Gravitational potential change
Cluster-centric IMBH
Larger number of ejections
Adiabatic or non-adiabatic encounters
Tidal or impulsive encounter
Hyperbolic or quasi-parabolic orbit
< 10 AU
> 10 AU
Planetary mass difference, e.g., planetary system architecture
$M_{larger\ planet} >> M_{others}$
Planetary separation

Deep-LPS

- Neural-network predicting code
- Orbits are predicted by the code
- Less precise than normal LPS
- Much, much faster (1000 to 100000 times) than LPS
- NOT a N-body code

~Myr

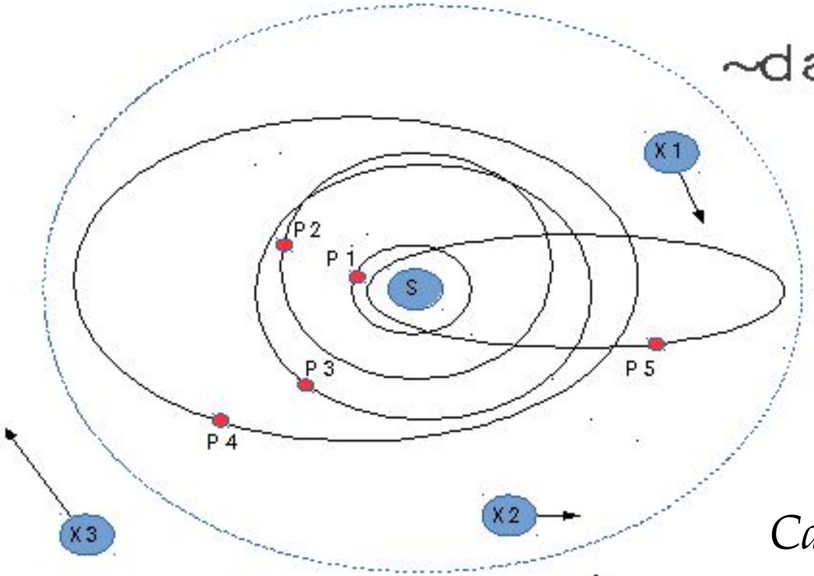

~days

Cai et al 2015

Technical Aspects

~kyr

Nb6++GPU-MPI

7th order splines

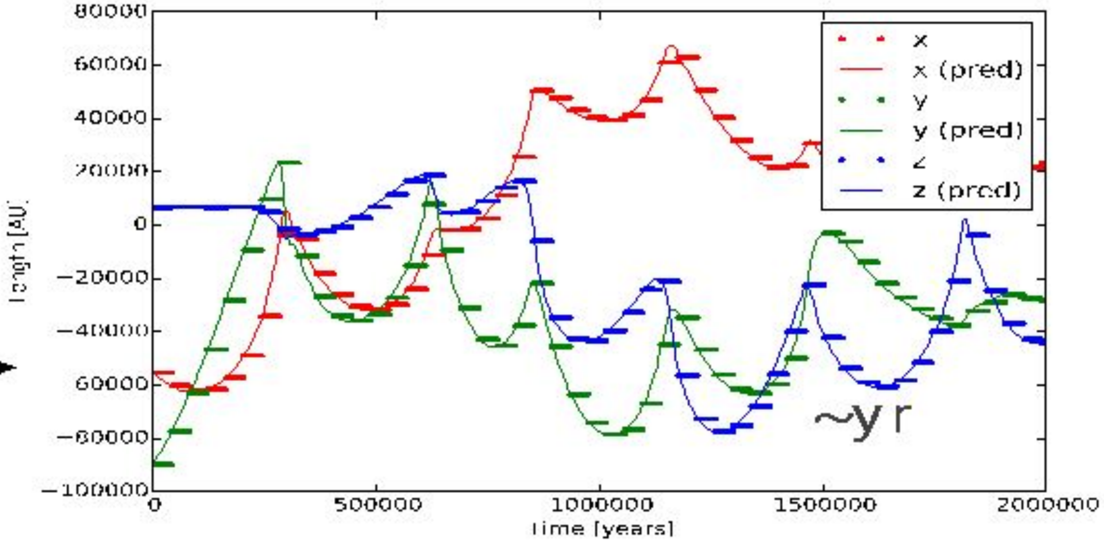

predictor-corrector scheme

Plummer model

$$\rho_P(r) = \left(\frac{3M}{4\pi a^3}\right)\left(1 + \frac{r^2}{a^2}\right)^{-\frac{5}{2}}$$

$M = 5000\ M_{sun}$

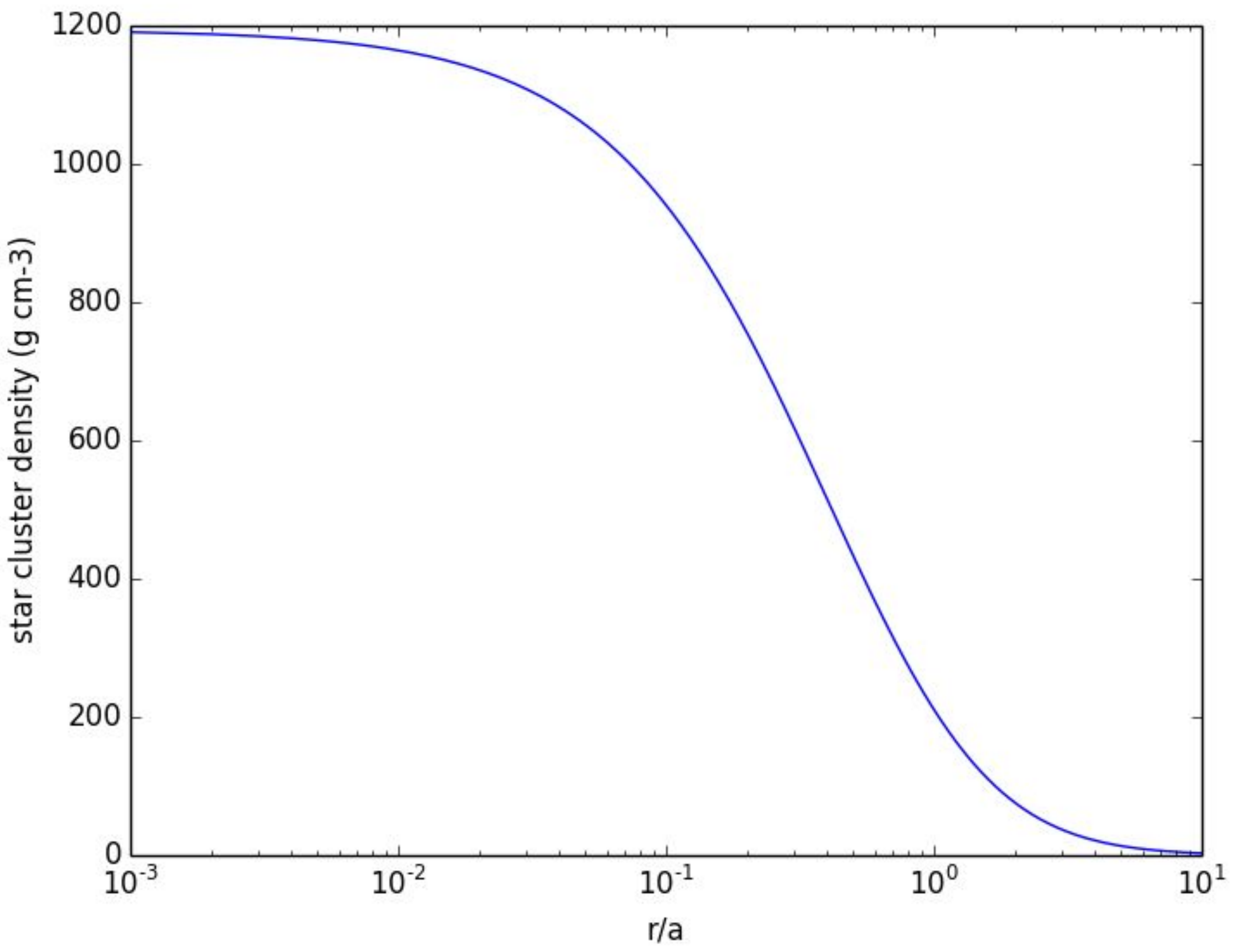

Advantages:

- It is easy to model
- Various astronomers had good result using this distribution on star clusters
- It represent most of the star cluster distribution

Disadvantages:

- It is not a good model for very big star clusters
- On the long distances from the center it loses accuracy
- It is bad for little open clusters

$$r = \sqrt{x^2 + y^2 + z^2}$$

$$\theta = \arccos \frac{z}{\sqrt{x^2 + y^2 + z^2}} = \arccos \frac{z}{r} = \arctan \frac{\sqrt{x^2 + y^2}}{z}$$

$$\varphi = \begin{cases} \arctan(\frac{y}{x}) & \text{if } x > 0, \\ \arctan(\frac{y}{x}) + \pi & \text{if } x < 0 \text{ and } y \geq 0, \\ \arctan(\frac{y}{x}) - \pi & \text{if } x < 0 \text{ and } y < 0, \\ +\frac{\pi}{2} & \text{if } x = 0 \text{ and } y > 0, \\ -\frac{\pi}{2} & \text{if } x = 0 \text{ and } y < 0, \\ \text{undefined} & \text{if } x = 0 \text{ and } y = 0. \end{cases}$$

We quantify the direction of escape using the angular momentum per unit mass, **h** = **r** ×**v**

We use the inclination and azimuth as i = arccos(hz / |h|) with i ∈ [0, 180◦], and the azimuth, α = arctan(hy /hx), with α ∈ [−180◦, 180◦]. 90 inclination is equator, 0 North pole and 180 South pole.

Stability of planetary systems in star clusters

1. Architecture of the planetary system:

   a. $M_{mms} >> M_{others}$
   b. Interplanet distance
   c. P(10 AU) (Fujii 2019)
   d. Distance from the star

$$p(M_p, a_p)\left(= \frac{dN}{dM_p da_p}\right) = 1.03 \times 10^{-2} \left(\frac{M_p}{1\ M_{Jup}}\right)^{-1.31} \left(\frac{a_p}{1\ AU}\right)^{-0.61},$$

2. Star cluster density in the inner regions

3. Encounter Strength:

   a. Periastron encounter <= planet semi major axis
   b. $V_{inf} \sim V_{orb}$
   c. $1 < e_{orb} < 2$

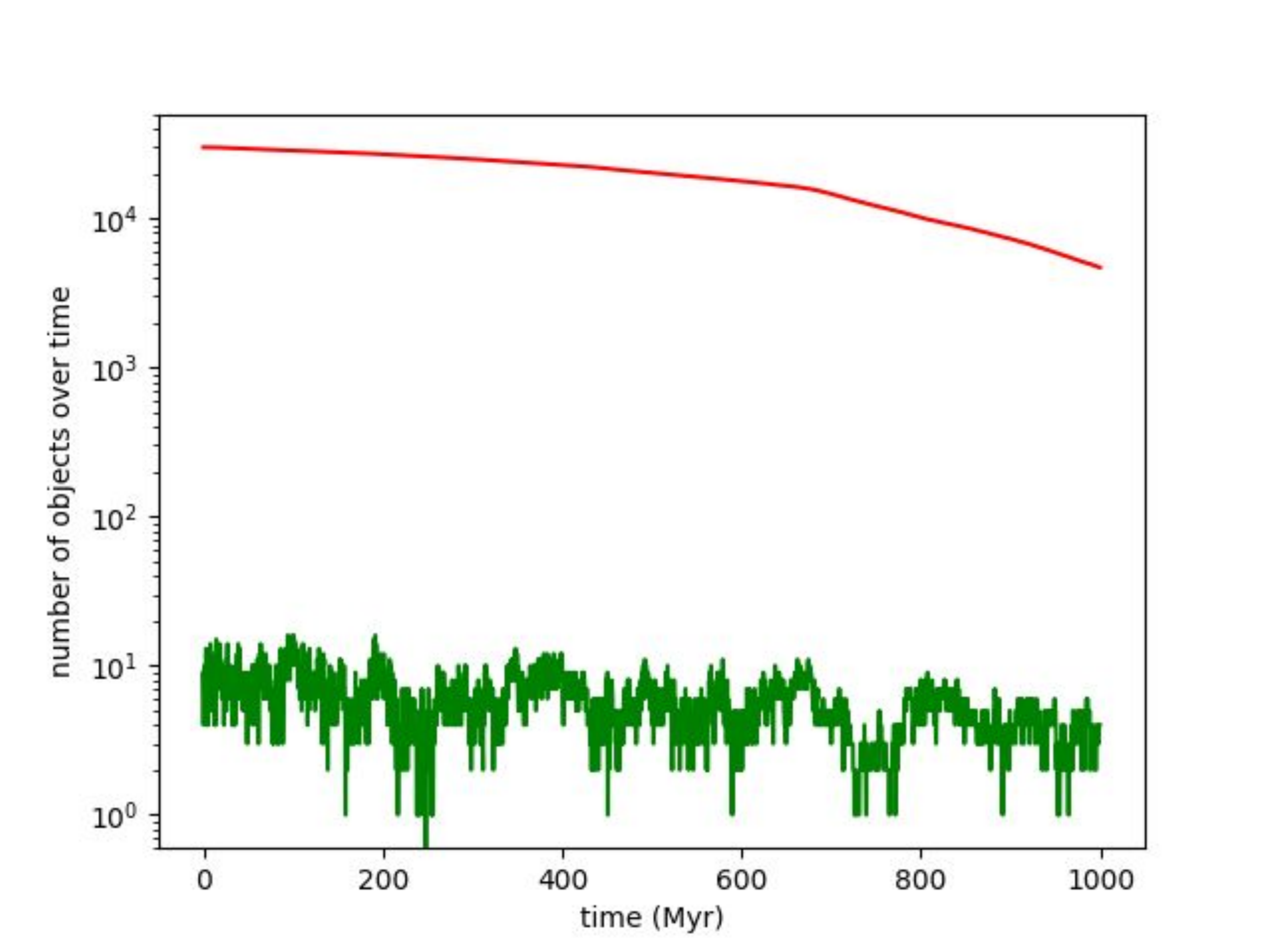

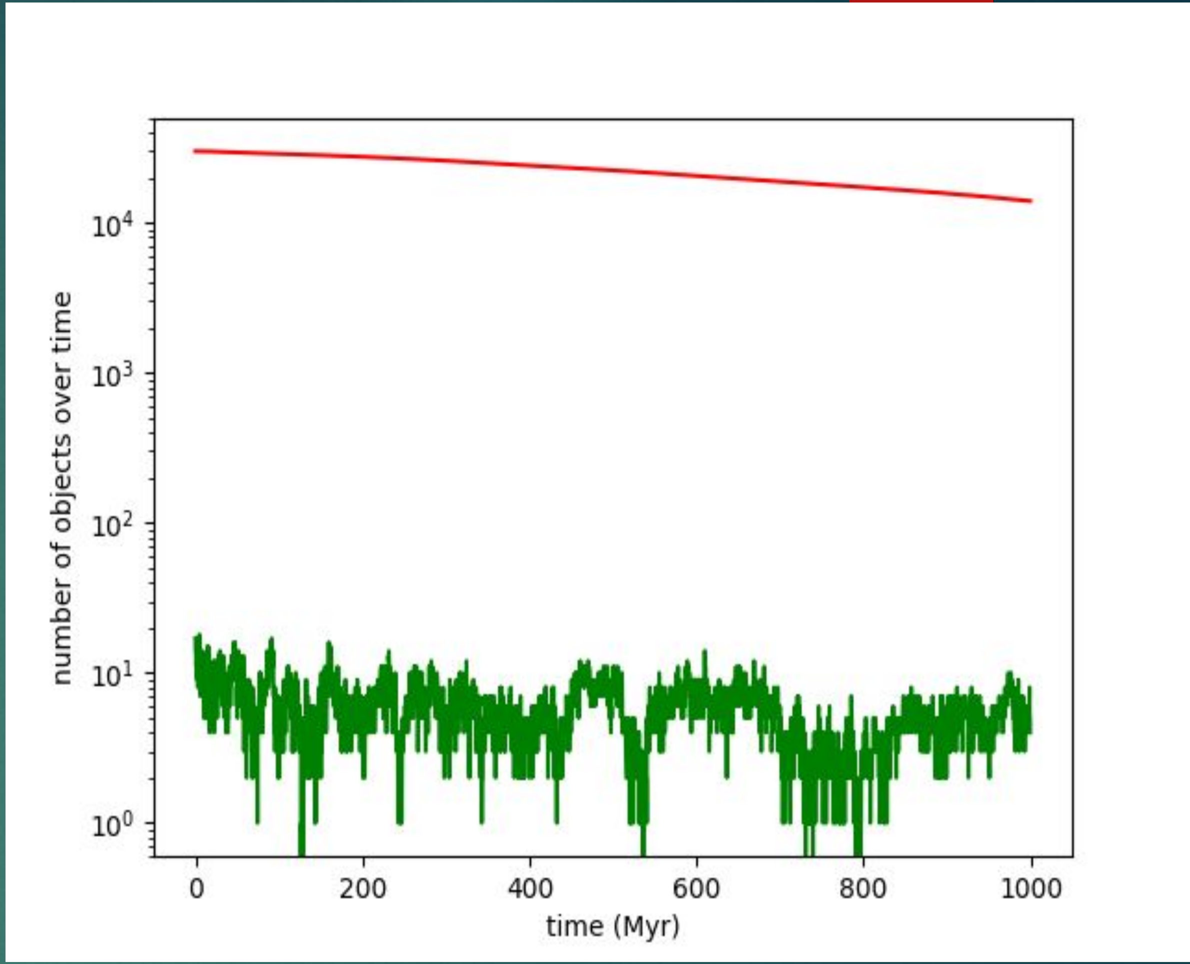

Green dynamical planetary systems, red surviving planets

Ejected components velocities

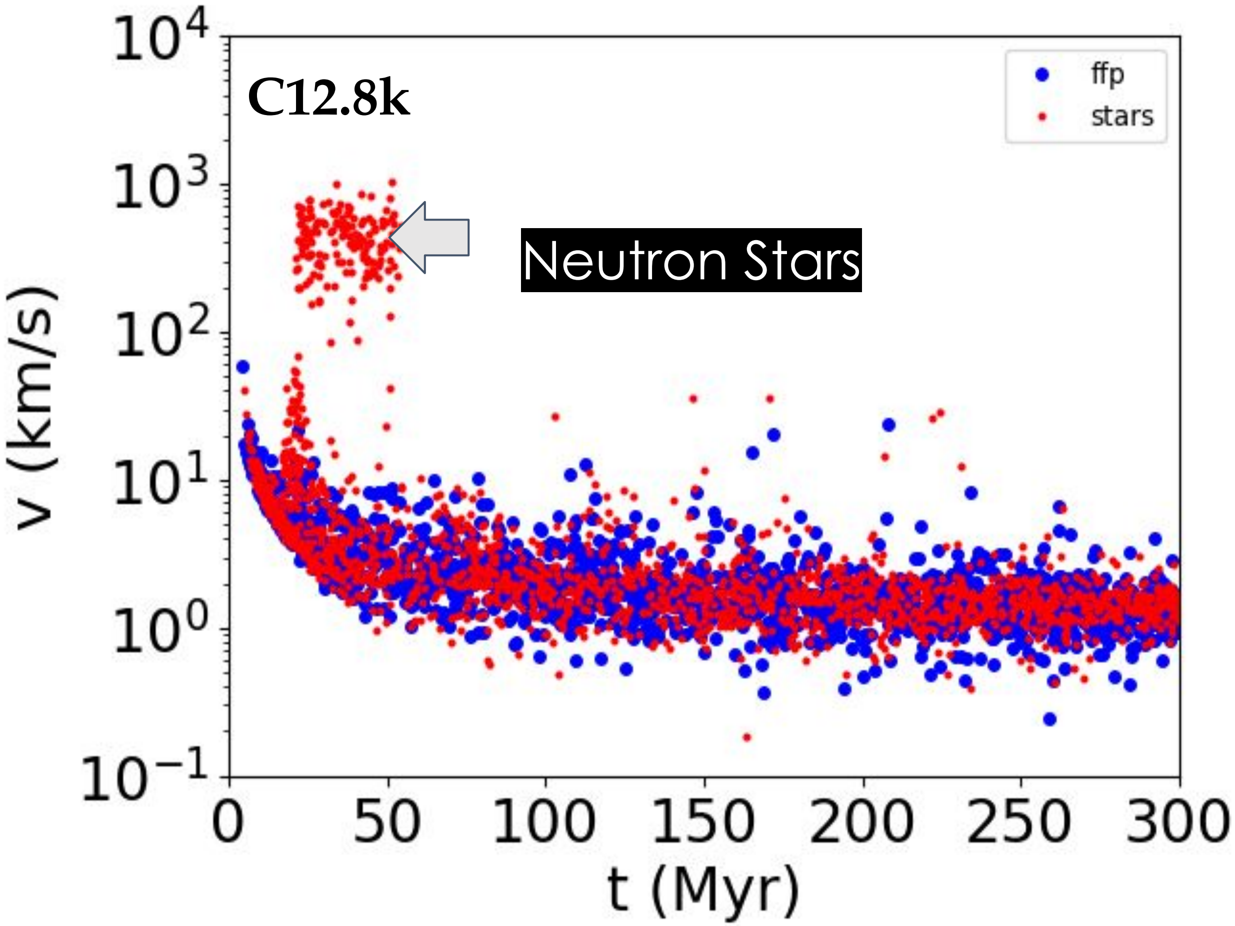

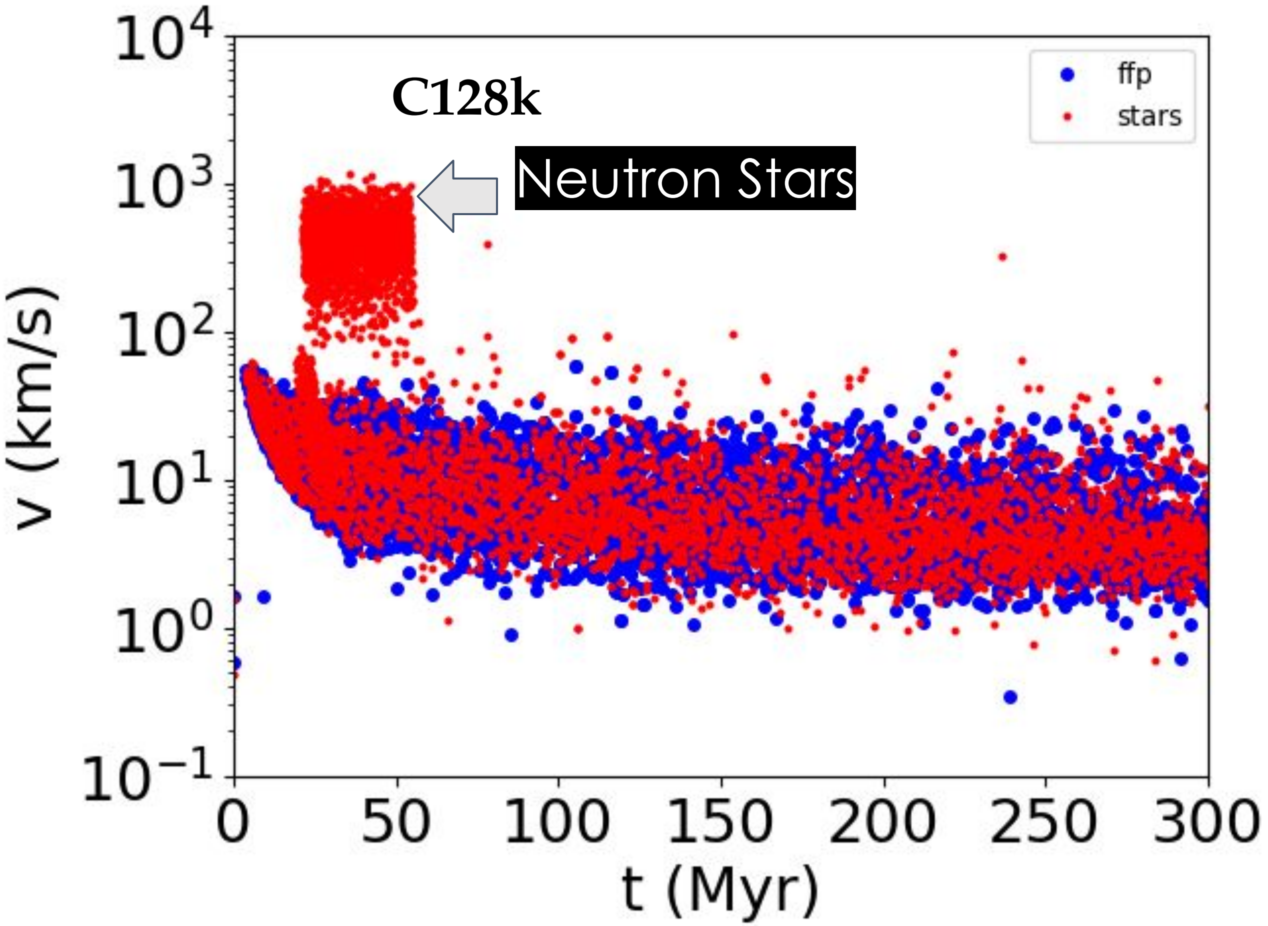

$\langle v_s \rangle$ = 3.86 km/s and 11.56 km/s

$\langle v_{ffp} \rangle$ = 2.83 km/s and 9.41 km/s

Table 4. The fraction of planetary systems with a certain number planets remaining in orbit around the star at time $t = 50$ Myr, for star cluster model C051E4. The majority of the planetary systems remain intact (6 planets), although they may be somewhat perturbed by encounters, while none of the planetary systems in this model lose all their planets.

Planets remaining	Fraction
6 planets	$88.5 \pm 2.3\,\%$
5 planets	$5.0 \pm 1.5\,\%$
4 planets	$1.0 \pm 0.7\,\%$
3 planets	$0.0^{+0.7}_{-0.0}\,\%$
2 planets	$2.5 \pm 1.1\,\%$
1 planets	$3.0 \pm 1.2\,\%$
No remaining planets	$0.0^{+0.7}_{-0.0}\,\%$

86.4 %
4.7 %
1.0 %
0.1 %
2.3 %
0.1 %

Curiosity: Terrestrial planets survive, most of them are still in the Habitable Zone

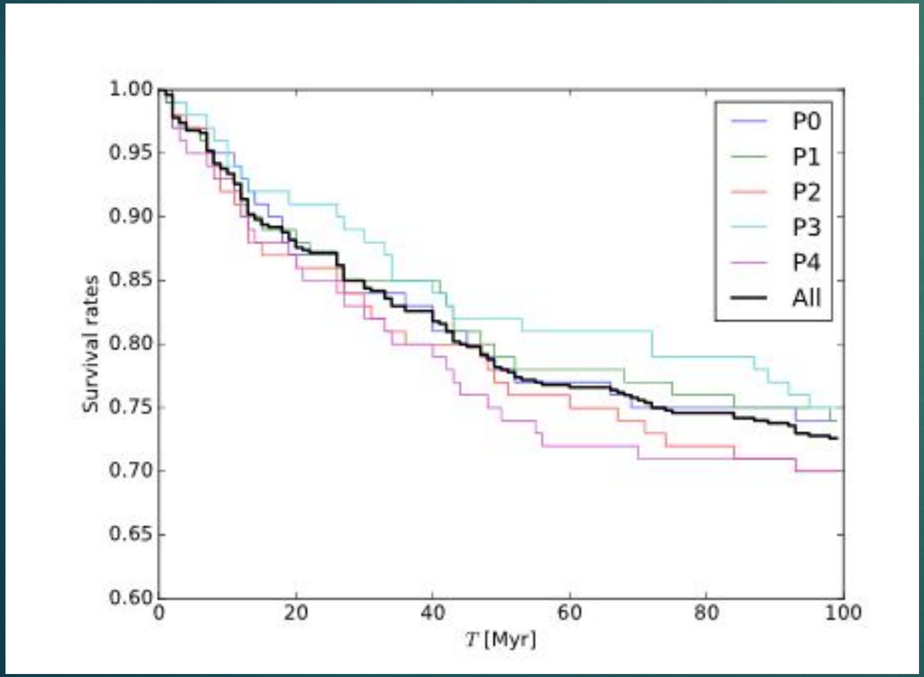

From Cai 2019, in a Young Massive cluster. The survival rate of equal-mass planetary systems is still high (~ 72 %)

Stability of planetary systems in star clusters

1. Architecture of the (single) planetary system:

   a. P(10 AU) (Fujii 2019)
   b. Distance from the star (Spurzem 2009 and many others)

$$p(M_\mathrm{p}, a_\mathrm{p}) \left(= \frac{\mathrm{d}N}{\mathrm{d}M_\mathrm{p}\mathrm{d}a_\mathrm{p}} \right) = 1.03 \times 10^{-2} \left(\frac{M_\mathrm{p}}{1\ M_\mathrm{Jup}} \right)^{-1.31} \left(\frac{a_\mathrm{p}}{1\ \mathrm{AU}} \right)^{-0.61},$$

2. Star cluster density in the inner regions

3. Encounter Strength (Spurzem 2009, Flammini Dotti 2019):

   a. Periastron encounter <= planet semi major axis
   b. $V_{inf} \sim V_{orb}$
   c. $1 < e_{orb} < 2$

Central IMBH in the cluster disrupt more planets and ejects more planets from the cluster, although this effect is mostly in the first Myrs (Flammini Dotti 2020b)

Black irregular forces, white regular, asterisk “reference star”

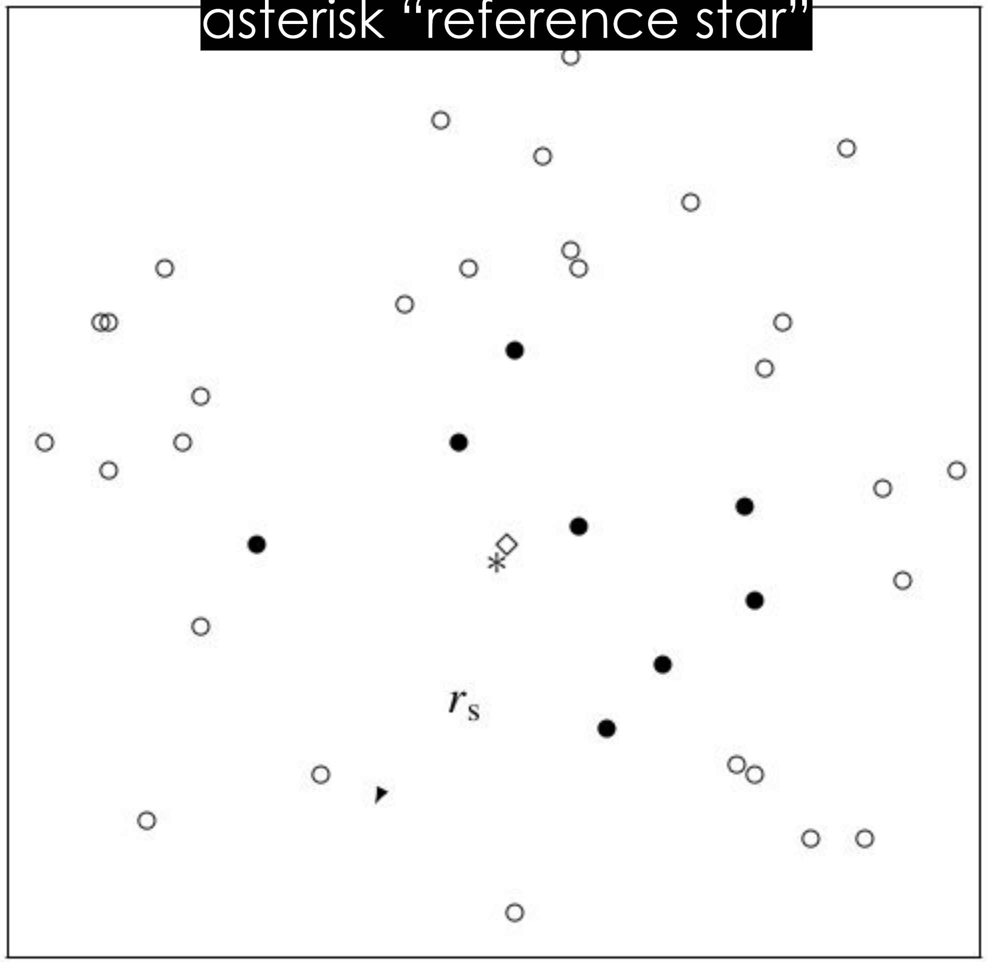

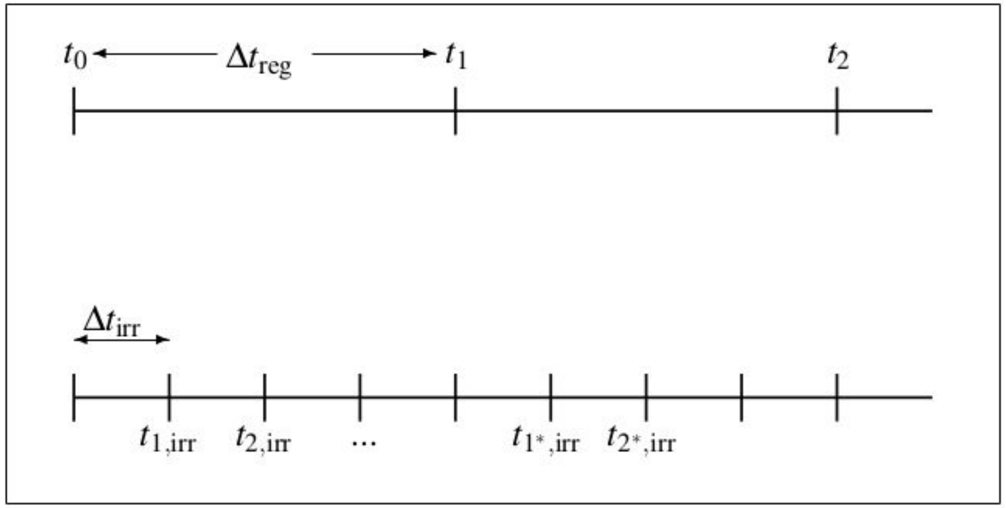

Figure 10.2: Regular and irregular time steps (after [22]).

$a_i = a_{i,reg} + a_{i,irr}$ for $N_{neigh} << N_{tot}$ is more effective (Ahmad 1973)

They are (KS) regularised in a binary, always as secondary

All of this with a single flag which depends on the mass of the planet (which is always much smaller than the stellar mass).

中国科学院国家天文台

the SILK ROAD PROJECT at NAOC

丝绸之路计划

GPU Cluste

JUWELS Boos

Golowood clus

Kepler/bwFor c

Max-Planck MP

Ki

UK

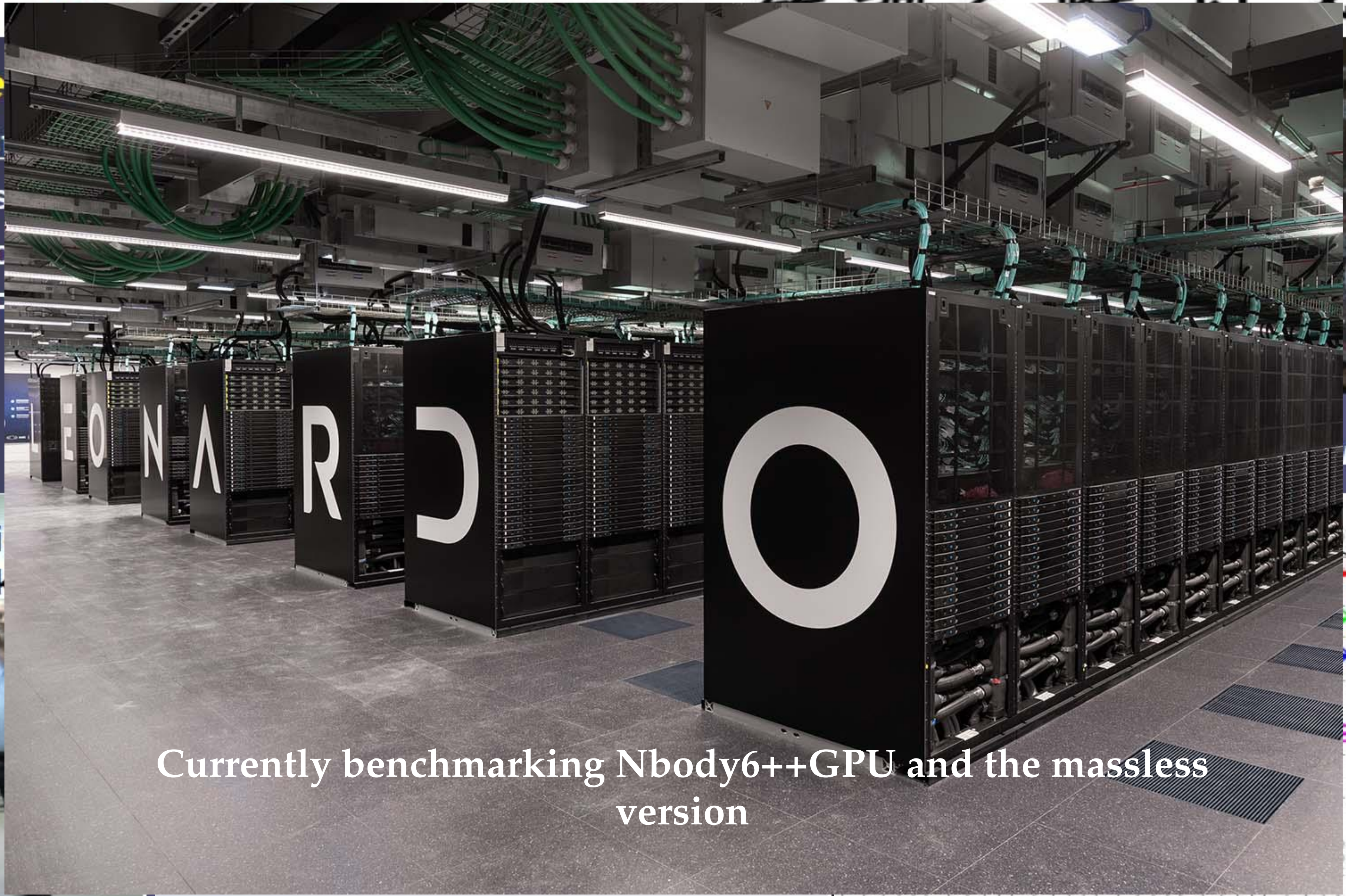

Currently benchmarking Nbody6++GPU and the massless version

PU N-Body

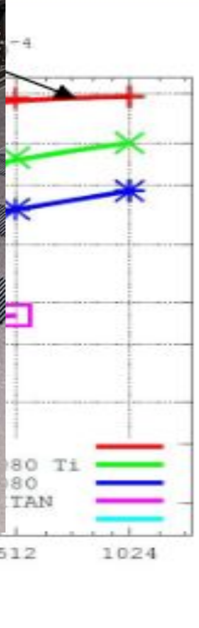

Lumi (Finland)

Ejected stars and massless particles

We quantify the direction of escape using the angular momentum per unit mass, $\mathbf{h} = \mathbf{r} \times \mathbf{v}$.

We use the inclination and azimuth as $i = \arccos(h_z / |h|)$ with $i \in [0, 180^\circ]$, and the azimuth, $\alpha = \arctan(h_y / h_x)$, with $\alpha \in [-180^\circ, 180^\circ]$. 90 inclination is equator, 0 North pole and 180 South pole.

ω_0	T_{rot}/T_{kin}
0.00	0.00
0.05	0.23
0.10	0.89
0.20	3.38
0.30	7.00
0.40	11.23
0.50	15.61
0.60	19.81
0.70	23.71
0.80	27.18
0.90	30.25
1.00	32.99

Model ID	$M_{cluster}$ $M_\odot$	ω_0	t_{cr} Myr	t_{rh} Myr	r_c pc	r_{hm} pc	Other parameters
C06w00	5.39×10^3	0.0	0.18	26.52	0.29	0.74	FFP $= 1000$
C06w03	5.39×10^3	0.3	0.18	27.87	0.32	0.77	$Q = 0.5$
C06w06	5.39×10^3	0.6	0.20	29.85	0.39	0.80	$r_{vir} \sim 1$ pc & 10 realisations

Table 2. Average fraction of all models of the escaping particles (stars and FFPs), at $t = 100$ Myr. In parenthesis, the total number of ejected particles of all iterations for each type of model.

Model ID	escaped stars	escaped FFPs
C06w00	2.91 ± 0.05 % (2913)	5.18 ± 0.22 % (518)
C06w03	2.86 ± 0.05 % (2869)	5.25 ± 0.22 % (525)
C06w06	2.59 ± 0.05 % (2596)	4.23 ± 0.20 % (423)

Ejection of planets is slightly lower than non-rotating models, but nevertheless quantifiable

Overall star and planets results

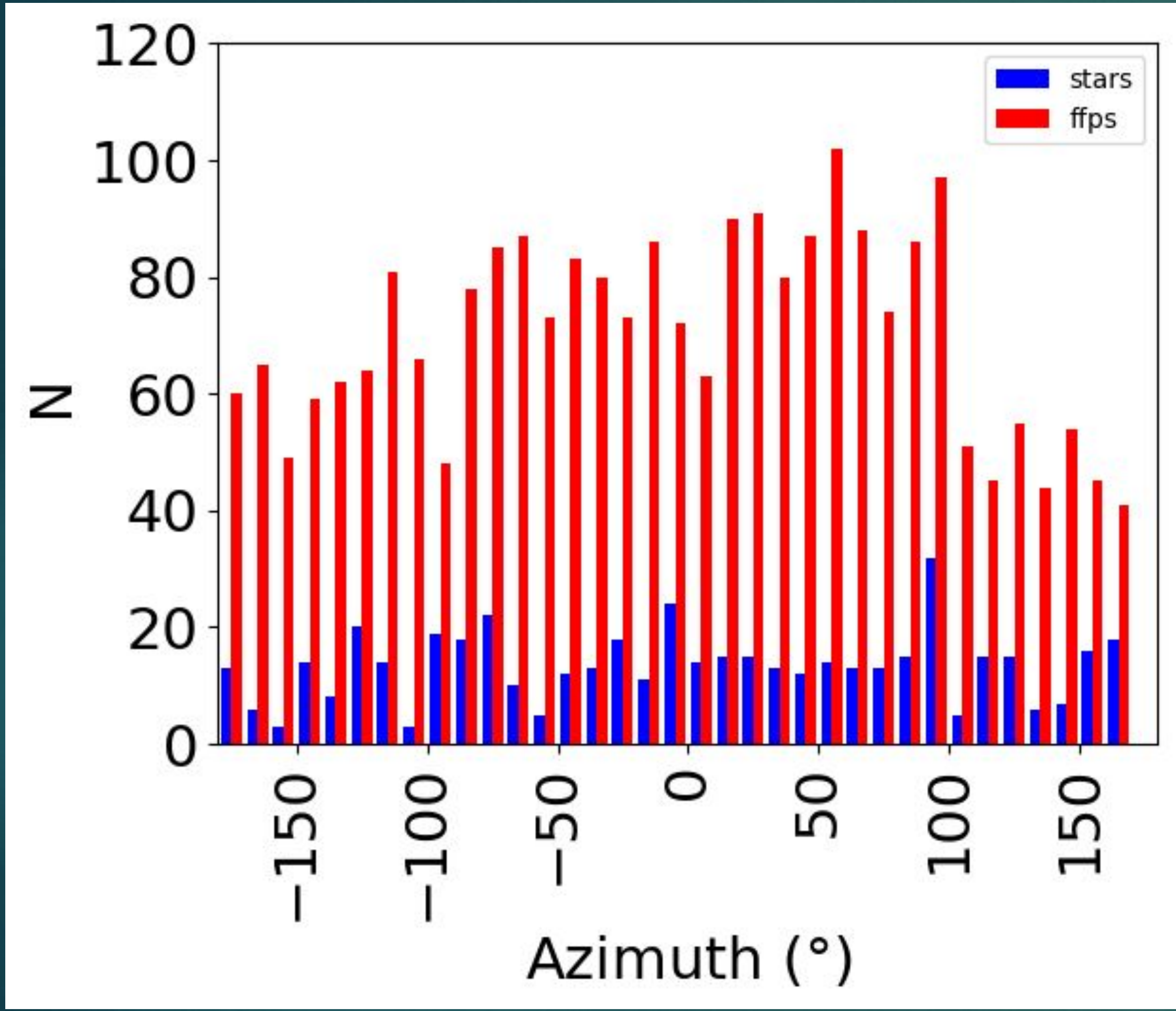

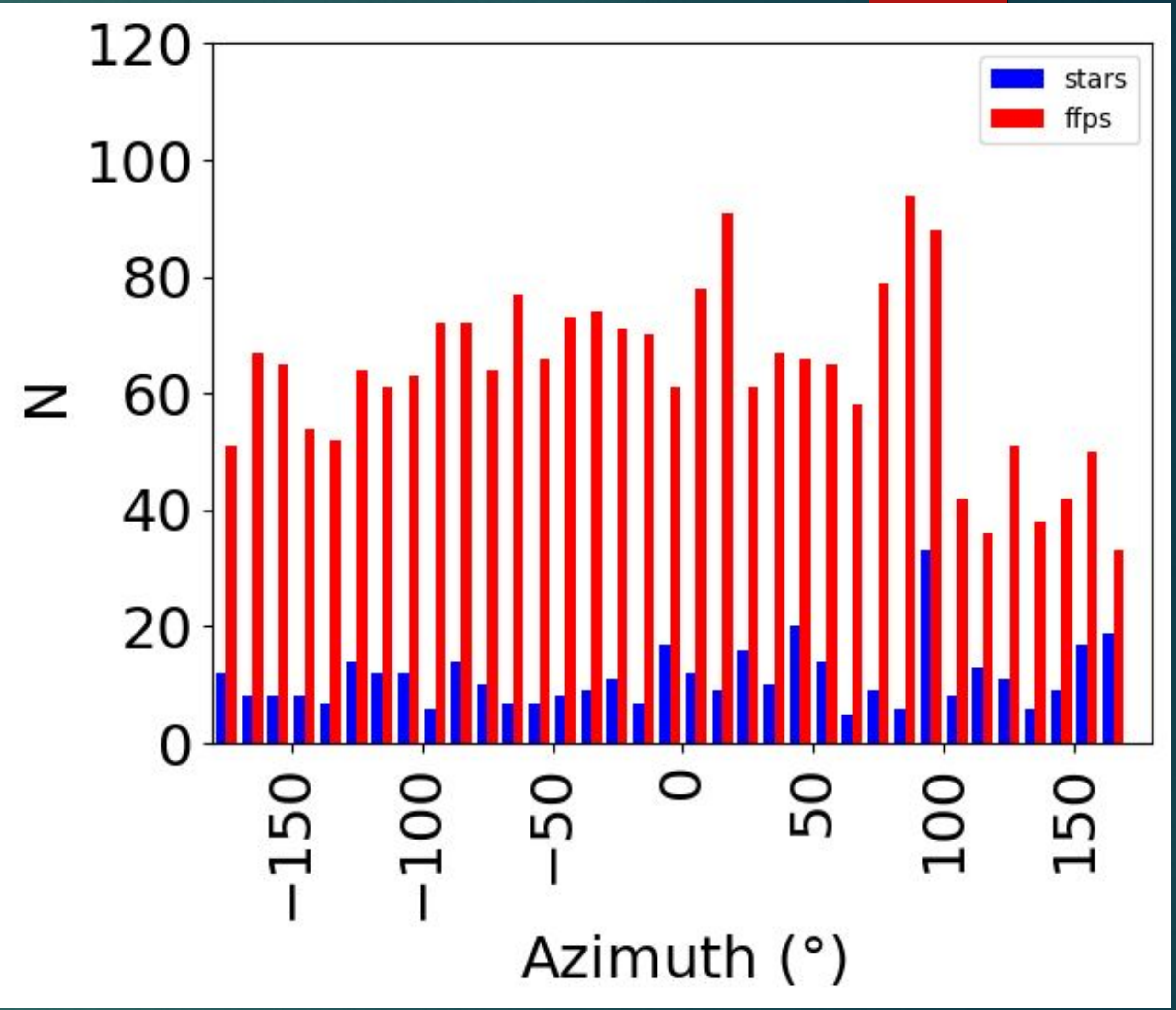

w0 = 0 w0=0.6

Overall star and planets results

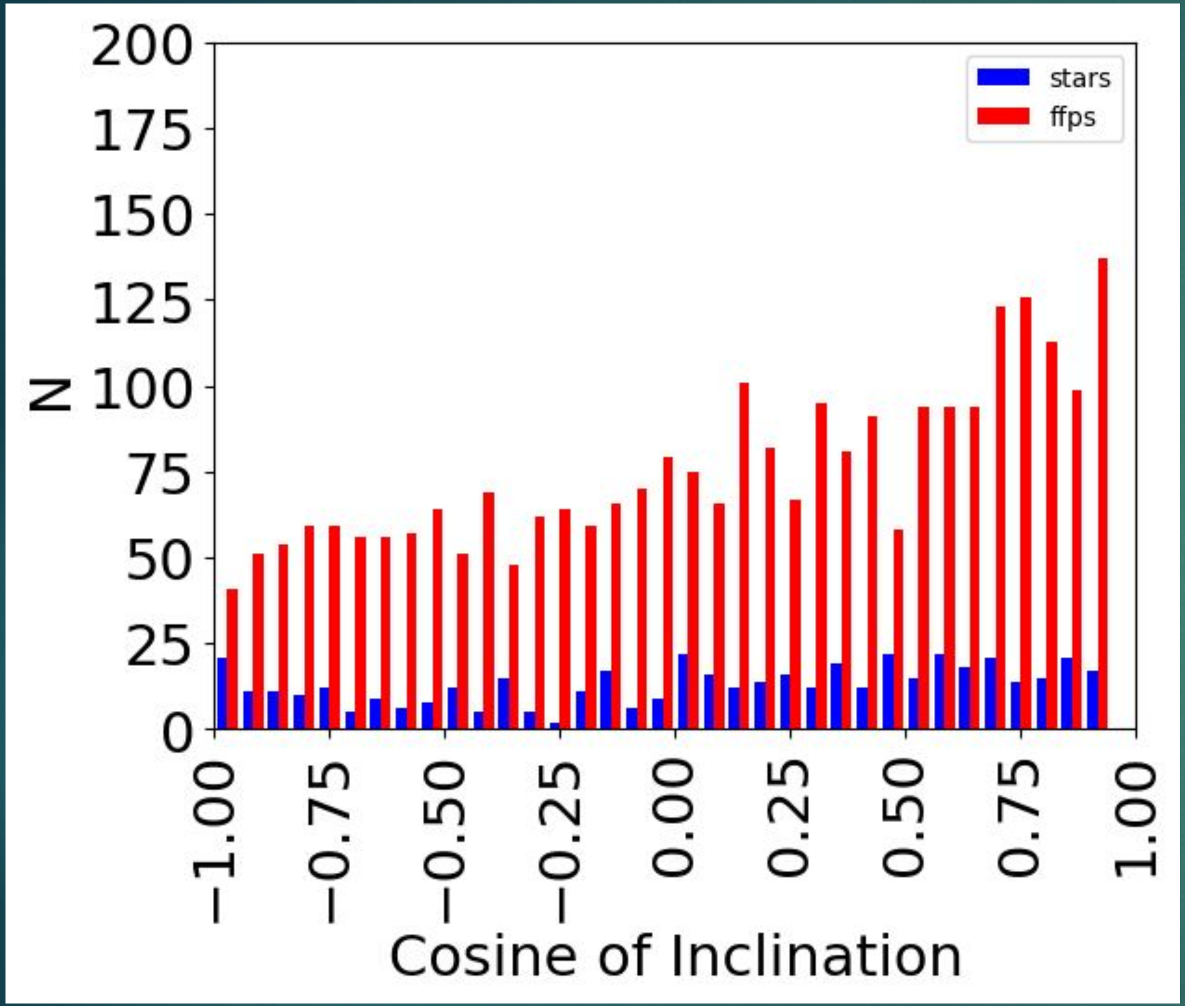

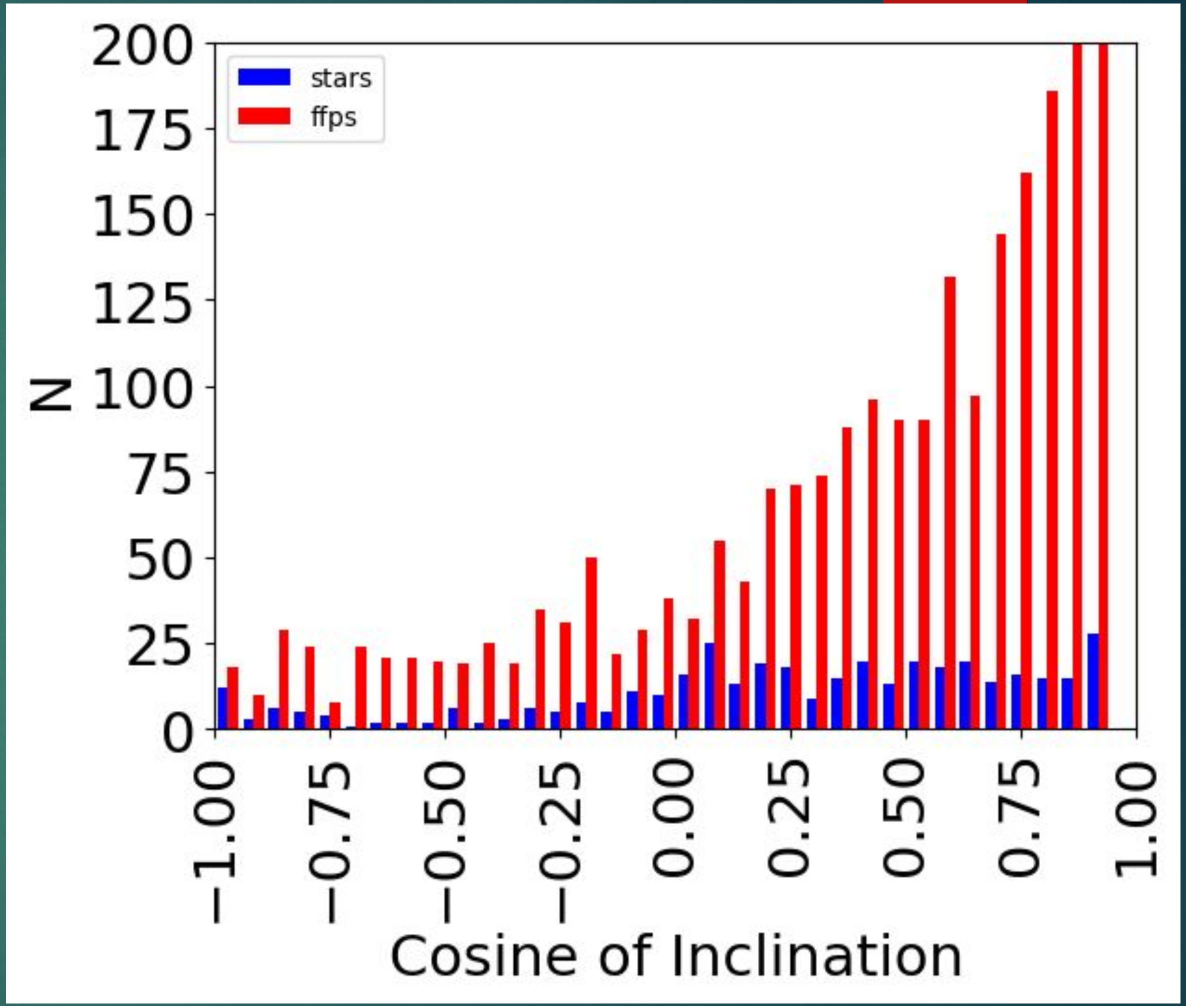

w0 = 0 w0=0.6